Sizing and Operational Analysis for Hybrid Electric Aircraft:
A feasibility study for the regional market

Yilin Deng*, Alexander Kryuchkov*, Paul R. Mokotoff*, Emma Smith[†], Janki Patel[‡], Santiago Garcia Lavanchy[‡], Max Z. Li[§], and Gokcin Cinar[¶]

Department of Aerospace Engineering, University of Michigan, Ann Arbor, Michigan 48109

This study establishes a foundation for evaluating hybrid electric aircraft (HEA) integration in commercial aviation, bridging the gap in the literature by addressing aircraft design, battery sizing, and operational aspects. The primary objective is to explore the feasibility and benefits of HEA in the context of airline operations, focusing on the regional market. A representative aircraft is identified through market analysis and historical flight data, and several HEA models are designed based on top-level aircraft requirements and design mission profiles. The performance of these HEA models is evaluated on actual, historical sequences flown by a commercial airline, comparing fuel burn benefits against a conventional aircraft. Key findings reveal that operating HEA at different levels of hybridization can achieve 1-5% fuel savings compared to conventional aircraft, contributing to energy efficiency and environmental sustainability goals. The most significant advantages emerge when HEA are operated on shorter range missions, indicating potential benefits for regional airlines. Some HEA configurations faced challenges in completing certain mission legs, but further optimization is possible. This paper serves as an essential stepping stone in the analysis and paves the way for a more extensive co-optimization problem, exploring the potential of HEA within commercial aviation.

I. Nomenclature

BTS	=	Bureau of Transportation Statistics
CRS	=	Computerized Reservations Systems
HEA	=	hybrid electric aircraft
ICAO	=	International Civil Aviation Organization
KPP	=	key performance parameter
LCC	=	low cost carrier
MTOW	=	maximum takeoff weight
NLC	=	network legacy carrier
OD-pair	=	Origin-Destination pair
PLF	=	passenger load factor
SAF	=	sustainable aviation fuel
SOC	=	state of charge
TLAR	=	top-level aircraft requirements
TOGW	=	takeoff gross weight
US	=	United States
VTOL	=	vertical takeoff and landing

II. Introduction

As the civil aviation industry continues to grow, CO_2 emissions have significantly increased in recent decades [1]. To prevent further environmental degradation, the International Civil Aviation Organization (ICAO) has established a

---

*Graduate Student, Department of Aerospace Engineering, University of Michigan, Ann Arbor, Michigan 48109, AIAA Student Member.

[†]Undergraduate Student, Department of Aerospace Engineering, University of Michigan, Ann Arbor, Michigan 48109, AIAA Student Member.

[‡]Research assistant, Department of Aerospace Engineering, University of Michigan, Ann Arbor, Michigan 48109.

[§]Assistant Professor, Department of Aerospace Engineering, Department of Industrial and Operations Engineering, University of Michigan, Ann Arbor, Michigan 48109, AIAA Member.

[¶]Assistant Professor, Department of Aerospace Engineering, University of Michigan, Ann Arbor, Michigan 48109, AIAA Senior Member.

long-term goal of net-zero emissions by 2050 for the global aviation industry [2].Efforts to achieve this goal include sustainable aviation fuel (SAF), optimizing air traffic management and other operational efficiencies, hydrogen fuel, and electrified aircraft. However, many alternative fuels face technical barriers: SAF can reduce CO_2 emissions by 80% but at high production costs [3]; hydrogen fuels have low volumetric energy density, are expensive to generate emission-free, and are not commercially available in vast quantities [4]. Although electric aircraft are a promising technology for reducing emissions, the limited specific energy of state-of-the-art batteries restricts their range [5], making fully electric aircraft an unsuitable replacement for current fleets. As a result, hybrid electric aircraft (HEA), which combine electric propulsion with traditional kerosene-burning engines, are considered a feasible solution for near-term emissions reduction [6, 7]. In addition to reducing air pollution, HEA offer potential fuel savings and noise reduction during takeoff [8].

This paper aims to investigate and model various operational modes and energy management strategies for HEA to analyze trends of fuel burn. Although HEA can significantly reduce emissions, their range and payload capabilities are limited due to the low specific energy of batteries compared to conventional fuel. Presently, short-haul flights often use twin-engine aircraft with ranges far beyond what is needed for these routes. HEA can replace these planes in the market and reduce fuel burn and CO_2 emissions. However, modeling HEA requires consideration of battery specific energy, size, and weight, which all impact aircraft range and payload capabilities. Depending on tradeoffs between twin-jet airplanes and HEA, some short-haul flights may feasibly and optimally (in terms of emissions reduction) be served by newly introduced HEA.

A. Literature Review

Recent studies have investigated various aspects of HEA, including clean sheet and retrofit design, operational considerations, and environmental impact.

Clean sheet design. Several studies have focused on the initial aircraft sizing and design optimization of HEA, which determines the masses of each component in the aircraft and the maximum engine power requirement [9–13]. Hoogreef et al. [10] combined a preliminary sizing technique for distributed-propulsion HEA with a refined Class-II weight estimating approach where energy consumption is evaluated using a mission analysis method. Cinar et al. introduced a flexible vehicle sizing, trade-off, and optimization capability for unconventional flying vehicles and advanced hybrid-electric propulsion system architectures [11]. The framework developed by Cinar in [14] is designed for early design phases, allowing for quick evaluations and customizable design optimization setups without requiring extensive definition of the vehicle. Other studies proposed methodologies specifically for light aircraft and vertical takeoff and landing (VTOL) [12, 13]. Finger et al. found that discrepancies between these methods were small, with approximately 1% in power-to-weight ratio and less than 4% in maximum takeoff weight (MTOW) [9].

Hybridization of existing aircraft. Wroblewski and Ansell [15] applied hybridization to an existing aircraft by implementing a HEA model to a conventional single-aisle Boeing 737-700 using publicly available data and the MATLAB Simulink environment. The simulator was configured for a generic mission consisting of ground roll, climb out to clear a 35 feet (ft) obstacle, climb, cruise, descent, approach, and landing segments, along with sufficient reserves for a loiter or 200 nautical mile (nmi) diversion to a nearby airport. The aircraft model mimicked that of a Boeing 737. In addition to the aircraft geometry, performance parameters were also included, such as the service ceiling, cruise speed, MTOW, and maximum energy weight. Even though their model was not energy-dense enough to complete the typical mid-range missions for a Boeing 737, Wroblewski and Ansell showed that with near-future, mid-future, and far-future battery technologies, they were able to reach the average distance covered by all global flights.

Operational considerations. Geis et al. [16], Cinar et al. [17, 18], and Hoelzen et al. [19] investigated the impact of operational considerations at the system level, as well as the impact of power and energy density on the operational strategy of HEA. Geis et al. found that the fuel required could be decreased by 3% when the propulsion chain was operated using optimum fuel consumption parameters as opposed to the default operation configuration[16]. Cinar et al. showed that significant fuel savings could be obtained by co-designing the aircraft, its propulsion system, energy and power management strategy and the flight operations [17]. Hoelzen et al. found that HEA in the regional aircraft category with a 350 nmi range could be cost-competitive compared to conventional fuel-consuming aircraft [19]. Shi et al. conducted fleet-level analyses on a hybrid turboelectric distributed propulsion regional jet, examining missions with different payloads, ranges, and hybridization schedules [20]. Their research included life-cycle cost and emission predictions, as well as a sensitivity analysis to study the impacts of assumptions on fleet life-cycle cost and emissions, providing insights on the potential benefits of hybridization.

Environmental impact. Jain et al.[21] and Scholz et al.[22] examined the environmental impact of HEA on fleet-level

as well as ground emissions during taxi, and non-emission environmental impacts related to aircraft operations. Jain et al. concluded that the introduction of a single-aisle HEA in 2035 could potentially result in lower fleet-level CO_2 emissions than the baseline case with just conventional aircraft, with a maximum possible decrease of 15.93% in terms of CO_2 emissions in the year 2065 [21]. Scholz et al. found that with a battery specific energy of 1500 Wh/kg and renewable electricity production, the design missions showed an improvement in climate effect in terms of SGTP100 (sustained global temperature potential with a time horizon of 100 years) of up to 11.4% compared to a conventional reference aircraft [22].

B. Research Objectives, Guiding Principles, and Rationale

In the literature review, it is apparent that the benefits of HEA are maximized when integrated into clean sheet designs, rather than as retrofits to existing aircraft. Additionally, incorporating energy and power management strategies during the design stage is crucial, as it significantly influences the size of the propulsion system and the aircraft itself, which in turn impacts fuel burn. Furthermore, previous studies do not address the integration of HEA into airline operations, specifically the operated sequences and ground turn times at airports, which is critical for charging. Consequently, the overarching goal of this research is to create a co-design and co-optimization environment for both aircraft design and operational analysis.

To fully exploit the potential of HEA, it is essential to optimize them in conjunction with fleet operations, including airline scheduling practices and considerations such as fleet ("which type of aircraft to operate on a given route?") and tail assignments ("which specific aircraft within a type to assign to a given route?"). This work establishes the foundations for a comprehensive computational framework that will enable the co-optimization of HEA systems with airline fleet operations, ultimately minimizing CO_2 emissions across next-generation aircraft fleets. Our ultimate objective is to integrate system design tools with operations modeling capabilities, allowing for iterative analysis. In this paper, we focus on rapidly and efficiently modeling HEA missions for commercial fleets. Our results reveal prototypical conditions under which aircraft electrification is feasible and beneficial for short- and medium-haul aircraft routes, which dominate the commercial aviation market in terms of emissions contributions [23].

Our previous research [17] delved into different hybridization strategies during the aircraft design process for the design mission. In this paper, we extend our focus beyond the design mission to consider existing airline operations. We investigate the short-haul segment by analyzing existing flight data from 2019 to identify a representative aircraft for our analysis. We then assess whether this representative, conventional aircraft can be replaced by an HEA counterpart capable of flying the same off-design missions (using an actual, historical sequence flown by a commercial airline) while providing fuel burn benefits.

In summary, this paper aims to present a comprehensive analysis of HEA in the context of both design and operations, highlighting the importance of co-optimization and identifying opportunities for further research and development in this area. By examining various scenarios and off-design missions, we seek to provide valuable insights into the feasibility and benefits of HEA for short- and medium-haul aircraft routes, setting the stage for more sustainable and efficient commercial aviation in the future.

III. Technical Approach

This research endeavors to model hybrid-electric aircraft operations and predict fuel burn trends for an aircraft serving the regional market. The methodology consists of a three-step approach with each step involving several analyses.

Step 1: Identify. The first step involves market analysis and selection of a representative aircraft. The market is surveyed to ascertain which routes could potentially be served by HEA as viable replacements for conventional aircraft based on data collected from the Bureau of Transportation Statistics (BTS) from 2019. This analysis centers on specific regional airlines operating under Network Legacy Carriers (NLCs), such as American Airlines and Delta Air Lines. Identifying the market shares that can be replaced by HEA is crucial for understanding their potential impact on reducing CO_2 emissions within the commercial aviation industry. Upon determining the available market shares, a representative aircraft fleet is selected for replacement by HEA.

Step 2: Design. In the second step, the representative aircraft and battery are designed for the regional market. The model of the representative aircraft is created using its top-level aircraft requirements (TLARs) and design mission profile from publicly available sources. Various energy and power management strategies are identified, and a set of HEA models are sized based on the same TLARs and design mission. This step involves two integrated and iterative analyses: aircraft sizing using an in-house sizing tool, and battery modeling and sizing. As a result, a set of HEA

models is obtained, which can be easily modified to model different technology levels and hybridization scenarios, thanks to the parametric nature of the inputs and assumptions. The sizing process is illustrated in the flowchart in Fig 1.
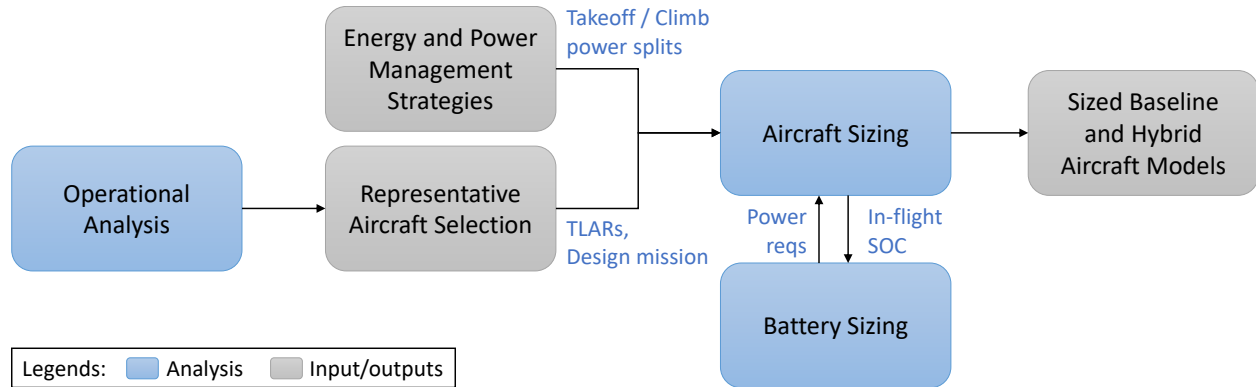

Fig. 1   Flowchart of the technical approach for aircraft and battery sizing analysis.

Step 3: Operate. The third step involves using the sized aircraft models in operational analysis, which consists of multiple stages. Route sequences, based on the 2019 BTS data, are analyzed for the representative aircraft. Each sequence consists of multiple flight missions flown back-to-back, with ground turn times at various airports in between. The varying ground times can affect the battery state of charge (SOC) at the beginning of each flight mission. The mission profile and predetermined power splits for each mission are provided by the operational analysis and energy and power management strategy blocks, respectively. The mission analysis block simulates the flight, returning the required fuel burn and final battery SOC. This iterative process continues until the fuel and takeoff gross weight (TOGW) values converge. The aircraft lands at the destination airport, and the operational analysis block sends ground time information to the charging analysis block. The battery is charged at a given rate for the entire duration of ground time, or until the battery SOC reaches 100%, whichever comes first. The new SOC becomes the initial SOC of the next flight mission. The operational analysis block sets the mission profile for the subsequent mission in the route sequence, and the process described in the previous steps is repeated for the new mission. This process continues until all missions in the sequence are simulated. The operational analysis process is illustrated in the flowchart in Fig 2. The output of this process is a detailed summary of the aircraft performance, including the mission history, fuel burn, and battery SOC as a function of time throughout the sequence. The subsequent subsections explain the methodology developed and followed for each of the above steps in detail.

A. Market Analysis and Identification of Representative Operations

Due to the intrinsic range limit of HEA caused by battery weight, it is not realistic for HEA to dominate the civil aviation network in the near future. Thus, a feasibility analysis is necessary to find the most promising market for HEA to permeate, in terms of operationally viability and optimal emissions reduction. Specifically, analysis is performed to find conventional aircraft for reference and HEA should then be designed to match the typical mission profiles and flight performance of these reference conventional aircraft.

The data is collected from the Bureau of Transportation Statistics [24]. Data in 2019 is selected because it is prior to the COVID-19 pandemic, hence the market was not affected by the pandemic. Some of the key parameters contained in the data sheet are number of departures performed, payload, available seats, passengers, distance, ramp-to-ramp time, air time, carrier (airline), origin airport, destination airport, aircraft group, and aircraft type, given according to each service (a service refers to all the flights provided by a carrier, with the same origin and destination and certain scheduled departure and arrival times).

There are some erroneous data points in the data sheet, potentially due to airline reporting mistakes or data entry errors. Thus, the data sheet was cleaned for the following outliers: flights longer than 9,000 miles or 18-hour airtime were removed. Then, flights with no range and no recorded departures were considered to be erroneous. Thus, they were also removed from the data set. Some of the BTS data metrics were aggregated across all flights made between a single origin-destination pair. As a result, the following parameters had to be divided by the number of recorded departures between that origin-destination pair: payload, passenger capacity, passengers flown, freight weight, mail
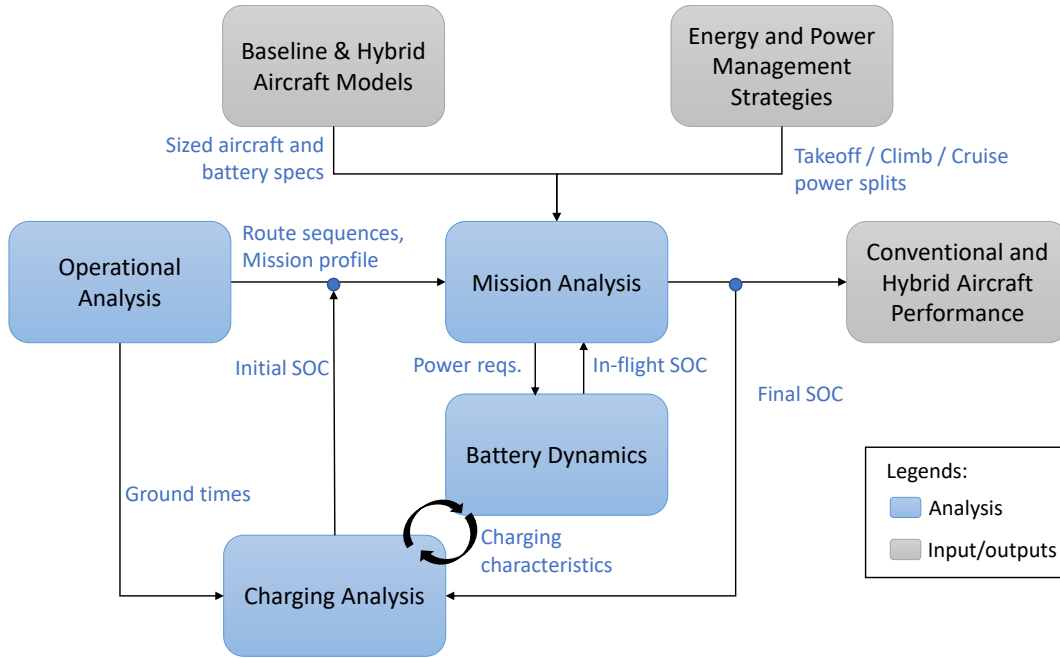
Fig. 2   Flowchart of technical approach for operational analysis.

weight, ramp-to-ramp time, and wheels-up to wheels-down time (airtime). Thus, average numbers for those metrics were obtained for all domestic US carrier flights. The BTS data also contained code numbers for the aircraft types used on a specific flight, as listed in Table 1.

Table 1   Aircraft group code numbers from the BTS data.

Code	Description
0	Piston, 1-Engine/Combined Single Engine (Piston/Turbine)
1	Piston, 2-Engine
2	Piston, 3-Engine/4-Engine
3	Helicopter/Stol
4	Turbo-Prop, 1-Engine/2-Engine
5	Turbo-Prop, 4-Engine
6	Jet, 2-Engine
7	Jet, 3-Engine
8	Jet, 4-Engine/6-Engine
9	Used for capturing expenses not attributed to specific aircraft types

The data from BTS was used to observe multiple flight operations trends with respect to five key performance parameters (KPPs). These KPPs were used to drive the TLARs for the representative HEA fleet:

1) Mission Range: the distance flown by the aircraft from its origin to its destination, measured in nautical miles (nmi).
2) Air Time: the wheels-up to wheels-down time, measured in minutes (min).
3) Passenger Capacity: the maximum number of passengers that could be flown on the aircraft.
4) Passenger Load Factor: the percentage of seats filled on a given flight.
5) Cruise Speed: the average speed flown by the aircraft to complete its mission, measured in knots (kts).

The gathered data was then used to show the most frequent KPPs for all domestic flights flown in the US. The

observed trends were used to target a significant portion of the short and medium haul markets that could potentially be hybridized. The flights were split into two groups: short-haul and medium-haul flights. A short-haul flight is defined as a flight with a range of 800 nm or less and an air time no longer than 270 minutes (min). Short-haul flights are operated by Part 121 airlines, also referred to as legacy carriers, and Part 135 airlines. Examples of Part 121 airlines include Delta Air Lines, American Airlines, United Airlines, and their associated regional carriers. On short-haul flights, Part 121 airlines fly both regional jets, such as the CRJ900 or Embraer E175, and single-aisle aircraft, such as the Airbus A320 or Boeing 737. Part 135 airlines are those that fly shorter routes between small cities or islands. For example, a Part 135 airline may fly passengers between two islands in Hawaii or between Juneau and Anchorage, two major cities in Alaska. Part 135 airlines commonly fly turboprop aircraft such as a Cessna Grand Caravan or ATR 42. A medium-haul flight is defined as a flight with a range between 800 and 2,200 nm and an air time no longer than 450 min. Medium haul flights are strictly flown by Part 121 airlines and primarily utilize single-aisle aircraft.

The plots presented reveal the flight operations trends associated with the TLARs found in the 2019 BTS data. First, the mission range and air time were plotted on a scatter plot. Figs 3a and 3b plot frequency and aircraft type, respectively, for all flights against their mission range and air time. The main aircraft contributors are turboprops and jets, represented as groups 4 and 6, respectively, in Fig 3b. In the figures, notice that there are two distinct bands that represent the most frequent flights, bounded by a blue or orange triangle. The band bound by the blue triangle encompasses ranges from 100 to 800 nm and flight times from 30 to 150 min, representing those flown by Part 121 airlines. The band bound by the orange triangle includes ranges up to about 300 nm and flight times from 30 to 125 min, representing those flown by turboprop aircraft under Part 135 airlines.

(a) The color bar represents $-\log_{10}$(Departure Frequency).

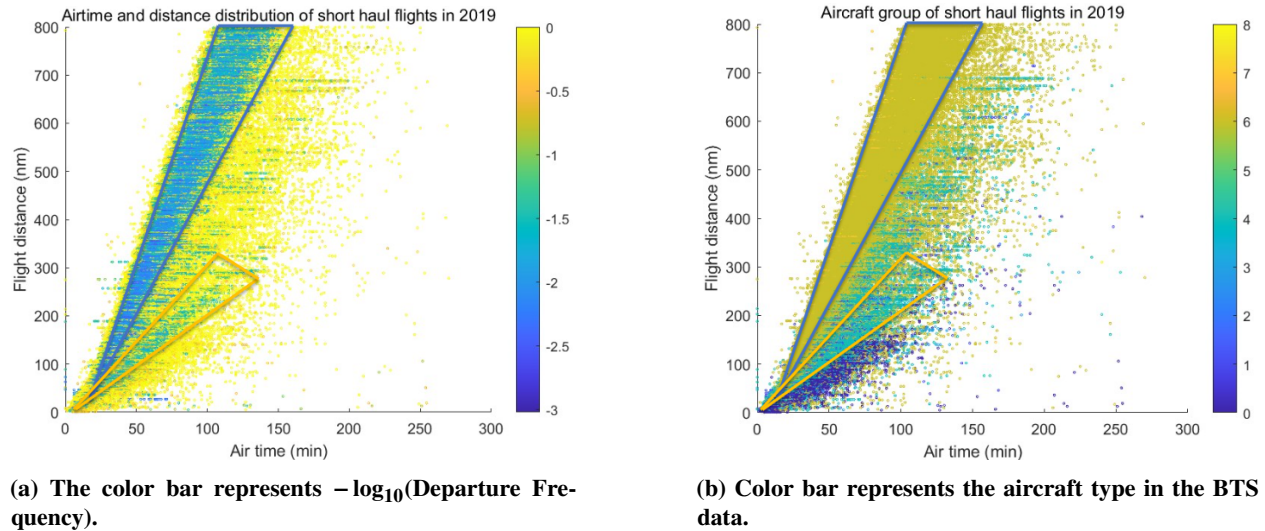(b) Color bar represents the aircraft type in the BTS data.

Fig. 3   Plots of the departure frequency and aircraft type against the mission range and air time.

For a constant mission range, the flight time varies based on the airlines' operating procedures. This provides a baseline of acceptable flight times that HEA must achieve in order to be competitive with the current aircraft fleet. For example, a flight takes two hours on a conventional aircraft and two hours, five minutes on a HEA. Since there is only a five-minute difference in the flight times, the airlines would likely be open to switching from a conventional aircraft to a HEA aircraft, at least from a block time perspective. In contrast, a flight takes two hours on a conventional aircraft and two hours, thirty minutes on a HEA. Since this is a 25% increase in flight time, the airlines would be less inclined to convert their existing fleet to one with HEA. Thus, in addition to satisfying the prescribed TLARs, the representative HEA must be competitive against the conventional aircraft fleet. The air time difference felt by the passengers is driven by cruise speed differences when modeling the HEA operations. In Fig 3b, it is obvious that airlines are now using twin-engine jets to fly missions ranging from 100 to 800 nm. As stated previously, aircraft flying ranges that are much shorter than their optimal design ranges results in further emissions, which motivates HEA to be a substitute aircraft type on these short-haul ranges.

Furthermore, in order to permeate the short and medium-haul markets, the representative HEA must be able to fly 80-90% of the missions. These cutoffs were chosen to represent a significant portion of the flight market. The cutoffs

will be used to determine the areas that could be permeated by the HEA aircraft. To determine these threshold values, histograms were made to further illustrate the flights associated with a given mission range. The histograms are plotted in Fig 4. In order to encompass 80-90% of the short-haul mission ranges, we are restricted to no more than 550 to 650 nm, respectively. Rounding up to account for mission reserves, a representative short-haul HEA must fly 700 nmi in order to be a viable replacement to the current aircraft fleet.
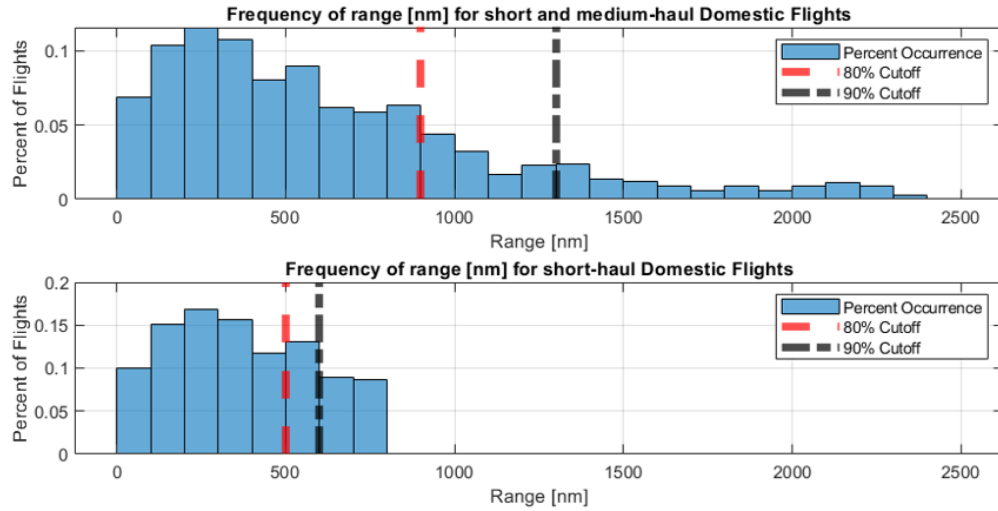

Fig. 4 **Histogram of mission ranges for all domestic flights and short haul flights only.**
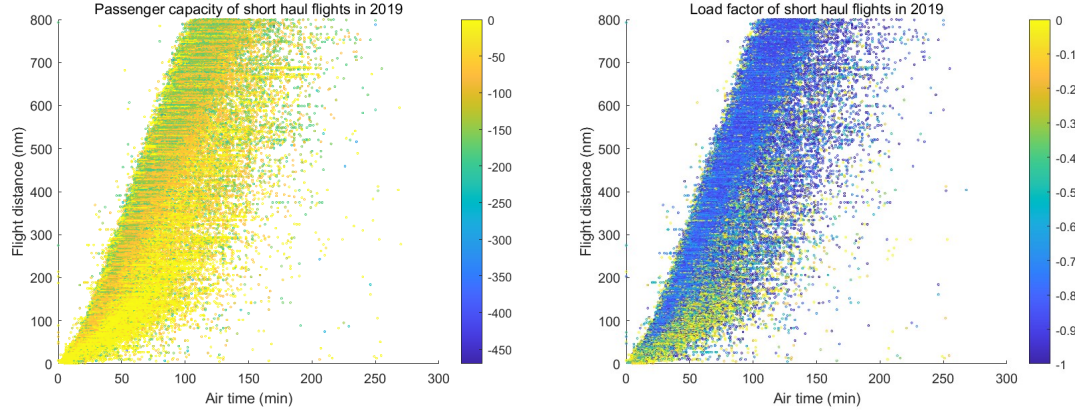
Aside from the threshold values for the short haul market, 80% of all domestic flights in the United States are no more than $1,000$ nm. Furthermore, about 50% of all domestic flights in the United States are no more than 500 nm, and fall within the required 700 nmi range that short-haul HEA must be able to fly. This highlights the vast market opportunities that can take advantage of potential HEA adoption.

Next, the passenger capacity and PLF were selected. Fig 5a and 5b plot the passenger capacity and PLF for all short-haul flights obtained from the 2019 BTS data against their respective mission range and flight time, respectively. Similar to the plots shown in Fig 3, there are two distinct bands. The green and orange in Fig 5a represent the flights primarily performed by legacy carriers and regional carriers with twin-engine jets, respectively. Legacy carriers tend to have higher passenger capacities than regional carriers. These same flights are represented in dark blue in Fig 5b. It can be seen that, despite the difference in passenger capacity, the load factors of these flights remain high. Thus, it is reasonable to conclude that routes within this region have sufficient demand. The light yellow areas in both Figs 5a and 5b show the flights performed by Part 135 airlines with turboprops (Fig 3b). The band bound by the red and black triangles represent flights flown by Part 121 airlines (twin-engine jets) and Part 135 airlines (turboprops), respectively.

For Part 121 airlines, the average passenger capacity of the twin-engine jets is on the order of 125 passengers and the average PLF is on the order of 0.85. Notice that this trend holds true regardless of the mission range, and signifies that the airlines will routinely fill their aircraft as close to their passenger capacity as possible. For Part 135 airlines, the average passenger capacity of the turboprops is on the order of 30 passengers and the average PLF is on the order of 0.25. Similar to the Part 121 airlines, this trend also holds true regardless of the mission range.

Next, the cruise speed was selected. Fig 6 is a histogram of the cruise speed for all short-haul flights obtained from the 2019 BTS data. The histogram reveals that 80% and 90% of all short-haul flights fly no faster than 360 and 380 kts, respectively. There are two distinct peaks in the histogram. On the right side of the plot, there is a large peak between 320 and 360 kts. This represents the nominal cruise speeds of twin-engine jets flown by the Part 121 airlines. On the left side of the plot, there is a smaller peak between 120 and 150 kts. This represents the nominal cruise speeds of turboprops flown by the Part 135 airlines. The peak representing the nominal cruise speeds flown by the Part 121 airlines is larger than that of the Part 135 airlines because the Part 121 airlines dominate the air transport system in the United States.

Lastly, in order to include HEA in the current civil aviation network, the airline operating procedures are taken into consideration in the following ways. First, it is well-known that network legacy carriers (NLCs) operate hub-and-spoke models. According to [25], aircraft operating to the closest spokes must wait for the return of aircraft from the most distant cities in order to meet the schedule of the upcoming inbound bank. As a result, these waiting time slots can

(a) Plot of passenger capacity. The color bar represents -(Passenger Capacity).

(b) Plot of PLF. The color bar represents -(PLF).

Fig. 5   Plots of the passenger capacity and load factor against the mission range and air time.
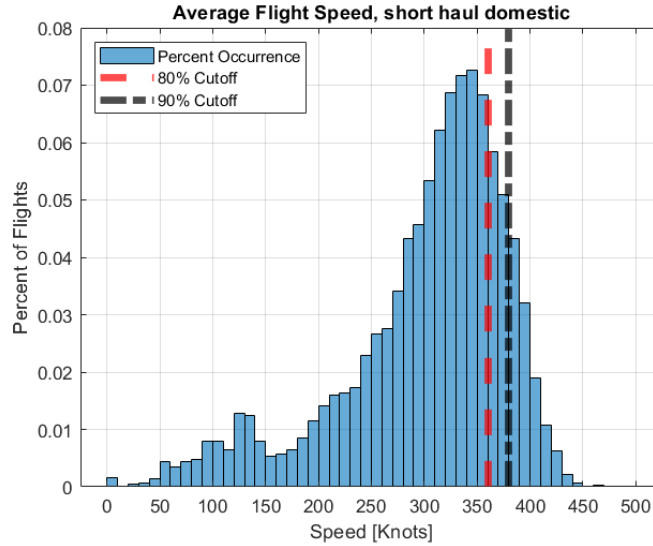

Fig. 6   Histogram of cruise speed for short haul aircraft.

be utilized for charging or replacing the batteries on HEA. Moreover, as reported by [26] and [27], some NLCs have publicly expressed their willingness to fly electric aircraft in their network in the near future, while low cost carriers (LCCs) have not. However, HEA will have stricter range limits due to the relatively low energy density of batteries, which might dramatically decrease the operational flexibility for NLCs when they swap their fleets at their hubs for medium and long haul routes. Combining the factors above, the subsidiary regional carriers serving as partners affiliated to NLCs, but mostly covering short haul routes, are a better market target for HEA to penetrate. Specifically for domestic flights within the United States, these airlines include Endeavor Air, Republic Airways, SkyWest Airlines, Air Wisconsin, CommutAir, GoJet, Mesa Airlines, Envoy Air, PSA Airlines, and Piedmont Airlines.

After filtering the BTS data sheet down to the routes performed by these subsidiary regional airlines, plots were generated to find their most frequently used aircraft types.

Figure 7 shows that Embraer ERJ-175, Canadair RJ-700, Canadair RJ-900, and Canadair RJ-200 cover most of the routes performed by the subsidiary regional airlines. These four types of aircraft are frequently used for almost all of the short-haul routes and even some medium-haul routes. Thus, it is reasonable to select these aircraft as representative
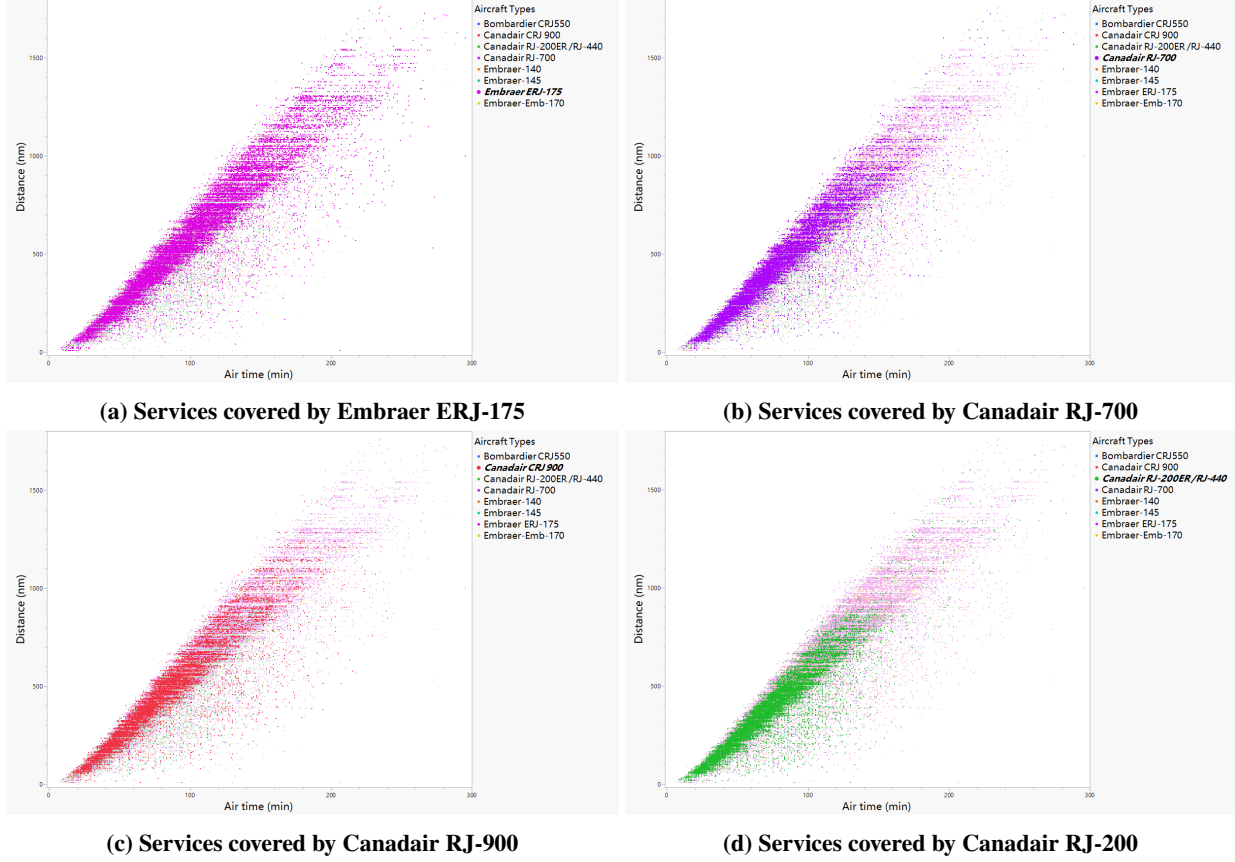
(a) Services covered by Embraer ERJ-175

(b) Services covered by Canadair RJ-700

(c) Services covered by Canadair RJ-900

(d) Services covered by Canadair RJ-200

Fig. 7   Plots of the routes flown by representative aircraft from subsidiary regional airlines.

reference aircraft.

B. Aircraft Operations Analysis

In order to include HEA in the future aviation network, it is essential to consider them in the context of the current aviation system, because being able to fly a single mission is far from enough. Ideally, the network should maintain the same passenger connectivity and airline operation flexibility with the introduction of HEA. Airline operation flexibility mainly manifests when airlines want to swap aircraft for different missions, which normally happens at their hub airports. As previously stated, the range of HEA will be limited due to the weight of batteries. Thus, it can be expected that airline operation flexibility will be decreased.

To ensure passenger connectivity, HEA should have similar ground time (turnaround time) at the airport gates as conventional aircraft have. While conventional aircraft spend ground time refilling their fuel tanks, HEA will spend the same ground time refilling and charging their batteries. This paper assumes that the batteries are charged on the ground, and in-flight battery charging is out of scope. Battery swapping at the gate is also left outside the scope of this paper due to regulatory concerns and uncertainties around an such activity. Thus, it is necessary to analyze ground time patterns of subsidiary regional airlines using data from [28].

An "OD-pair" or Origin-Destination pair refers to a direct flight route from an origin airport to a destination airport. Understanding the OD-pairs served by an airline and the associated ground times are crucial in planning the integration of HEA into the network. Ground time is the period an aircraft spends at the gate between flights, which for an HEA, would be used for battery charging. The number of services refers to the number of flights performed by a specific aircraft in a given period.

The ground time between two flights is defined as the time the aircraft spends at the gate. Specifically, in conjunction with two flights, an aircraft lands, taxis in, arrives at the gate, leaves the gate, taxis out, and takes off. The ground time is

the time between gate arrival time and gate departure time. Using the datasheet from [28], ground times for each flight are calculated by the difference between the Computerized Reservations Systems (CRS) arrival times and departure times, which are the times that aircraft arrive at or leave the gate. For all the first flights of a day, the ground times are assigned to be 0, and it is intuitive that there is enough time to charge the aircraft for the first flight of the day since the aircraft would stay at the gate overnight. For the later sequential flights, the ground time is calculated as the CRS departure time of the next flight minus the CRS arrival time of the previous flight.
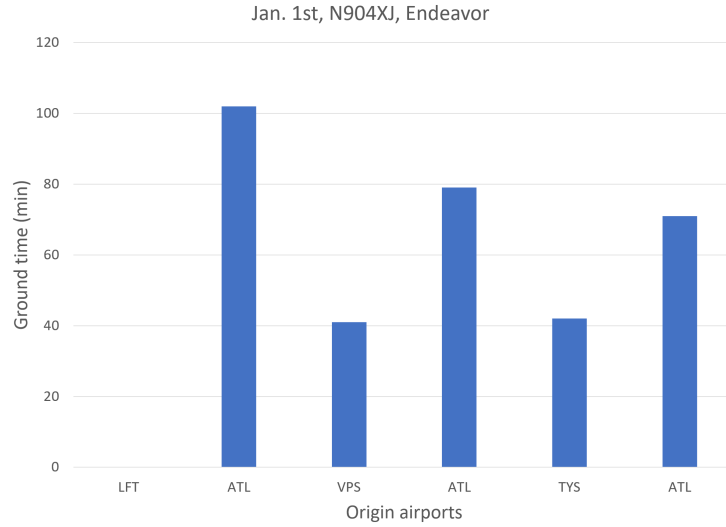

Fig. 8   Ground time calculation for N904XJ on Jan 1st

Figure 8 shows the calculated ground times of the tail N904XJ on Jan 1st, 2019 as an example. It can be seen in the figure that the tail N904XJ, operated by Endeavor Airline, started from Lafayette, LA, stopped by Atlanta, GA, Valparaiso, FL, Atlanta, GA, Knoxville, TN, Atlanta, GA, and stopped at Charleston/Dunbar, WV (which is not shown in the figure because this figure only includes the origin airports of the sequence, where ground times can be calculated) at the end of the day. Apparently, the operation of N904XJ on Jan 1st followed the hub-and-spoke model and as the hub airport of this sequence, ATL had much longer ground times compared with other airports.

In the broader context of future aviation networks, the successful integration of HEA goes beyond the ability to fly a single mission. The ideal scenario is to maintain the same passenger connectivity and airline operation flexibility that exist with conventional aircraft. To maintain passenger connectivity, HEA should have similar ground times as conventional aircraft. While conventional aircraft refuel during this time, HEA would also need to recharge their batteries.

C. Battery Model

When developing a hybrid-electric aircraft, accurate sizing and modeling of a battery system play an essential role in optimizing the performance of the aircraft, its efficiency, and its operations. As the battery supplies power to an aircraft, it contributes significant weight to a potential design. Therefore, a high-fidelity model of battery discharging and charging is necessary to reduce weight and increase the performance of an aircraft. The discharging and charging of a battery are treated separately since those two have different models, so considering them separately will increase the accuracy of the representation of how those systems work. Ultimately, this will result in an improved and more accurate design of an aircraft.

From an operations perspective, accurate battery modeling is vital for HEA integration into the existing management and logistical framework of an airport. The charging model of a battery will help estimate the amount of time required to charge an HEA while it is at the gate. Long charging times could disrupt the current departure schedule for airlines. At the same time, a battery that charges quickly could be too small to significantly increase the efficiency and performance of an aircraft.

Figure 9 shows the discharge and charge curves. The blue curve is the discharge curve, and the arrows point in the

direction of the curve when the battery is discharged. The red curve is the charging curve, which again follows the direction of the arrows (from right to left). A common assumption is to consider voltage to be constant throughout the discharge and charge of a battery. Here, however, it can be seen that voltage changes when the battery is either fully charged or fully discharged. Moreover, there are some differences between the discharging and charging models of the battery, specifically, the gaps between the two curves in the exponential and nominal zones. Those differences are small for a single cell, but when a battery is scaled, they could become crucial in determining the state of charge of an HEA battery.
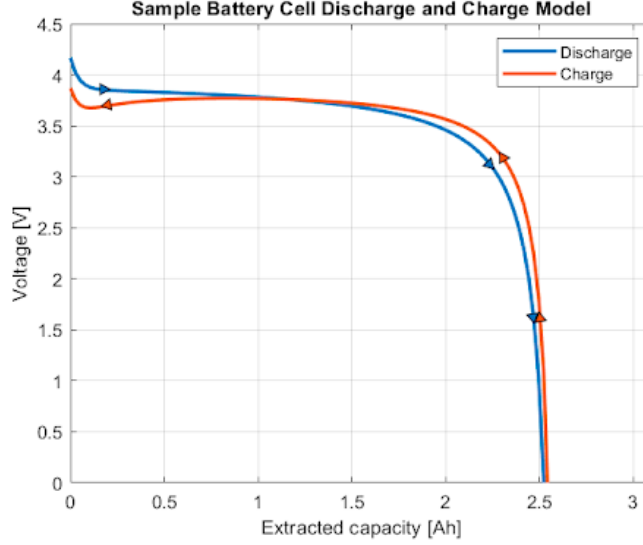

Fig. 9   Discharge and charge models of a cell of a battery.

There are four important features of the model. The extreme of the model on the left is the fully charged voltage V_{full}. The other extreme is the place with the maximum capacity Q_{max}. The remaining two points that Tremblay and Dessaint define are the end of the exponential zone and the end of the nominal zone. The end of the exponential zone is defined by V_{exp} and Q_{exp}; it is the zone where the curve ends its exponential behavior at the beginning of discharge. The end of the nominal zone is defined by Q_{nom} and V_{nom}; it is the zone where the voltage starts to decrease significantly.

Equations 1 and 2 show the equations for battery discharge and charge respectively:

$$V_{batt,discharge} = V_0 - R * I - K \frac{Q}{Q - Q_{act}}(Q_{act} + I^*) + A e^{-B * Q_{exp}} \tag{1}$$

$$V_{batt,charge} = V_0 - R * I - K \frac{Q}{Q_{act} - 0.1Q} I^* - K \frac{Q}{Q - Q_{act}} Q_{act} + A e^{-B * Q_{exp}} \tag{2}$$

where V_{batt} is the battery voltage, V_0 is the battery constant voltage, Q_{act} is the actual battery capacity, and I^* is the filtered current. The polarization constant K, the exponential zone amplitude A, and the exponential zone time constant B are defined in the equations 3, 4, and 5.

$$K = \frac{-V_{nom} + V_0 + A e^{-B * Q_{nom}}(Q - Q_{nom})}{Q(Q_{nom} + I)} \tag{3}$$

$$A = V_{full} + Vexp \tag{4}$$

$$B = \frac{3}{Q_{exp}} \tag{5}$$

The internal resistance R of a cell is assumed to be constant. Also, the temperature and aging effects are neglected.

Figure 10 shows the comparison of connecting cells in series and in parallel. In short, cells connected in parallel add to the capacity of the overall battery while cells connected in series add to the overall voltage of the battery. Thus, a scaled battery could have both enough capacity and voltage, which could be adjusted separately.
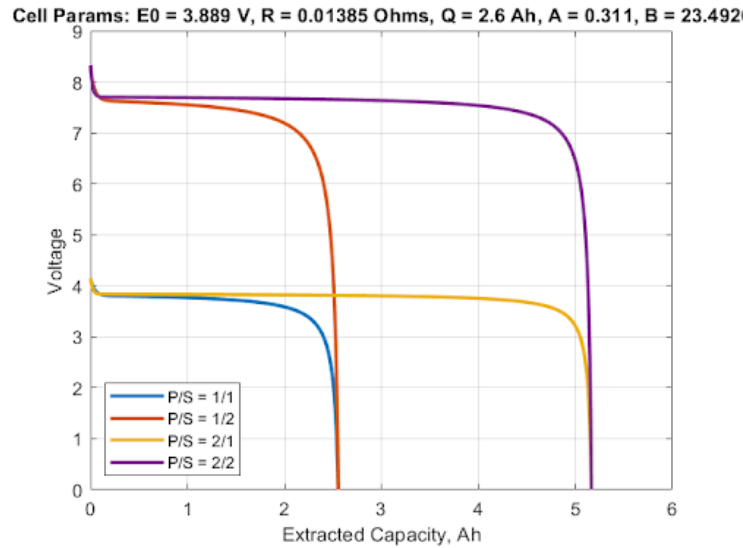

Fig. 10   Comparison of cells connected in series and in parallel to a single cell.

1. Role of the Battery Model in Integration

The battery model serves as a critical component in determining the overall weight, size, and performance of a hybrid electric aircraft. The model takes into account several inputs, including the required power, time of usage, initial charge level, and the initial guess for the size of the battery. Those are then processed to help determine the power available from the battery and its final state of charge, which is then used for the sizing of the battery.

For the purpose of integration, the number of cells connected in series in kept constant to keep the voltage of the battery at about 240 V. The number of cells connected in parallel, however, is what primarily determines the weight of the battery. Using the specific energy of the battery, the weight of the system can be calculated, providing weight value for the aircraft sizing process.

To ensure the optimal size of the battery is selected, the state of charge of the battery is used. If the state of charge of the battery drops below 20%, the battery size is increased accordingly to maintain a sufficient amount of charge. If the battery is too big, however, i.e., when the state of charge is above 23%, the battery is sized down accordingly. Eventually, the weight of the battery is expected to converge, which will determine the optimal weight of the battery for a specific aircraft design.

2. Power levels for charging

The power levels for charging were primarily based on currently available technologies. Based on the report by Le Bris et al. [29], the currently available charging rate available is 400 kW/h while a more common power rate is around 150 kW. Therefore, 150 kW/h was considered to be taken as a moderate estimate for currently available technology while the 400 kW/h charging rate was also considered as the state of the art technology currently available. Future power technologies such as 1 MW/h were not considered to avoid speculation and uncertainty of the development of such technologies and the timeline of their introduction. The currently available technologies show what can be implemented now to introduce the HEA to the modern aircraft missions.

D. Mission Analysis

In order to simulate HEA operations, a mission analysis was developed to fly a given route specified by the aircraft operations module. There are two main reasons why the mission analysis is essential to this research.

First, the mission analysis is used to estimate the required energy needed by the aircraft to fly the entire mission and allows for the aircraft's energy sources – battery and (kerosene) fuel tank – and other aircraft components to be sized. Given that HEA incur a weight penalty for carrying a battery, the mission analysis must accurately compute the battery's size and energy that it must store. Additionally, any energy not provided by the battery must be provided from fuel. If the energy that the battery supplies is not modeled accurately, then the energy supplied by the fuel won't be estimated correctly, thus leading to an improperly-sized aircraft.

Second, the mission analysis is used to track the aircraft's performance throughout the duration of the flight. This is done by computing performance parameters such as distance flown, altitude, airspeed, and rate of climb as well as other parameters of interest like the battery's state of charge (SOC, the percentage of charge remaining in the battery), aircraft weight, and fuel burned. As previously discussed, once the battery's SOC reaches 20%, it can no longer discharge or else permanent battery damage is risked. Also, by modeling the SOC as a function of time, various power-management strategies can be tested to understand which one minimizes HEA fuel burn. This will be of particular interest, especially in the cases that the aircraft's battery must supply energy for more than one flight between successive charges.

Additionally, the mission analysis is useful for estimating the weight fractions associated with each segment [14]. While the weight fractions for HEA will be different than conventional aircraft, they are useful for checking that the mission analysis functioned correctly. This was particularly helpful when testing verification cases involving conventional aircraft.

This paper employs a simplified version of the energy-based mission analysis approach presented in [14]. This approach emphasizes the segments where hybridization is most beneficial, specifically takeoff and climb, by discretizing them into multiple points. At each point, aircraft thrust is calculated based on the energy height. The remaining segments, including cruise, descent, and landing, are represented by the Breguet-range equation (BRE), which has been modified to accommodate hybrid electric aircraft.

The chosen approach, as opposed to using the BRE method for the entire mission, enables the utilization of different power splits, thereby allowing the hybridization of flight segments at varying rates. The advantages of employing varying power splits have been discussed in detail in Cinar [17]. In summary, modeling each segment separately makes it possible to assign a power-split on a segment-by-segment basis, which is a more realistic representation of how a HEA would be flown. Consequently, the energy provided by the battery will be computed more accurately, leading to a more reasonably sized aircraft. Additionally, having separate power splits for each mission segment offers greater control over the HEA's battery usage and facilitates experimentation with different power-management strategies.

At each point in the mission analysis, the aircraft has an energy height, H_e, as shown in Equation 6 as defined by Anderson [30].

$$H_e = h + \frac{1}{2g} \left(V_\infty\right)^2 \tag{6}$$

where h, V_∞ is the aircraft's altitude and speed, respectively. The energy height represents the aircraft's total mechanical energy – the sum of potential and kinetic energies – normalized by its current weight. Differentiating Equation 6 with respect to time yields the time rate of change of the aircraft's energy height:

$$\frac{dH_e}{dt} = \frac{dh}{dt} + \frac{V_\infty}{g}\frac{dV_\infty}{dt} \tag{7}$$

where dh/dt and dV_∞/dt are the rate of climb and acceleration, respectively. Equation 7 will be useful once the energy-based mission analysis is introduced next.

The energy-based mission analysis is based on a conservation of energy statement, as shown in Equation 8 [14].

$$TV_\infty = DV_\infty + W\frac{dH_e}{dt} \tag{8}$$

where the power provided by the engines (left-hand side) must match the power required to overcome drag at a given speed and the power required to change energy heights (right-hand side). In other words, any power available that isn't being used to overcome drag – the excess power – can be used to either: (1) climb to a higher altitude; or (2) accelerate to a faster airspeed. Once the rate of climb and acceleration are selected for each point in the mission, Equation 8 can be reformulated to compute the required power at each point in the mission:

$$P_{req} = DV_\infty + W\frac{dH_e}{dt} \tag{9}$$

13

In addition to knowing the required power at each point, the time to fly between points in the mission is also computed. Thus, the total energy required to fly the mission is:

$$E_{req} = \sum_{i=1}^{n} \left(P_{req} \right)_i \Delta t_i \tag{10}$$

here n is the number of points in the mission profile. For HEA, the power required is split between the battery and fuel (based on the user-prescribed power split for that segment), thus yielding separate energy requirements that the battery and fuel must provide.

Figure 11 illustrates the computational procedure for the abridged energy-based mission analysis. In general, each segment runs its own aircraft performance calculations and estimates the energy required to fly the segment using Equations 9 and 10.
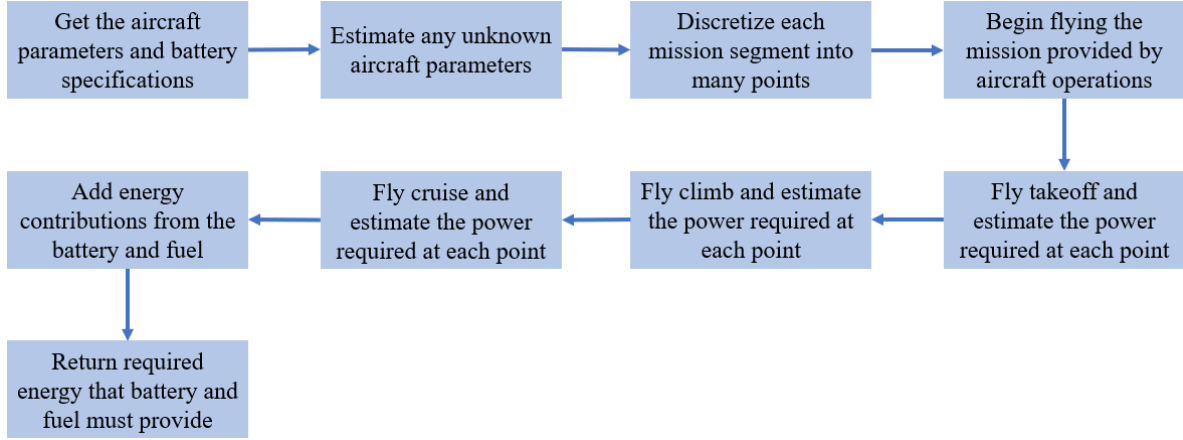

Fig. 11   Computational procedure for the mission analysis.

E. Aircraft Sizing

Aircraft sizing plays a pivotal role in designing a representative aircraft and battery for the regional market, as it estimates the key parameters that define an aircraft's size, weight, and performance capabilities. The purpose of aircraft sizing is to develop an aircraft design that meets the top-level aircraft requirements (TLARs) of the reference aircraft identified during market analysis. These requirements encompass mission requirements such as range, payload capacity, and speed, as well as point performance requirements. In this work, the point performance requirements were assumed to be matched by maintaining the thrust-to-weight ratio (T/W) and wing loading (W/S) of the baseline aircraft across different configurations.

Aircraft sizing in this study is conducted using an iterative procedure that continually refines the aircraft's weights and size based on the TLARs and an initial guess provided as input. This process is illustrated in Fig 12. The blue cells in the figure represent pre- and post-processing steps, while the green cells represent the steps taken during the sizing iteration. This aircraft sizing procedure delivers an optimized aircraft design that meets the TLARs while minimizing weight and determines the necessary propulsion system size, fuel and battery capacity, structural weight, and other critical parameters that impact an aircraft's overall performance and operational capabilities.

IV. Results and Discussions

This section presents a comprehensive analysis of the performance and feasibility of HEA models in comparison to the notional ERJ-175 reference aircraft. This analysis is conducted through a systematic application of the three-step approach, considering various modeling assumptions such as power split variations, battery technology levels, design range, and battery charging rates. The impact of these assumptions on the feasibility of HEA operations and the benefits in terms of fuel burn reduction are thoroughly investigated, revealing trends in fuel burn and battery SOC for different operating conditions. The feasibility of HEA operations is determined by the availability of sufficient battery energy at
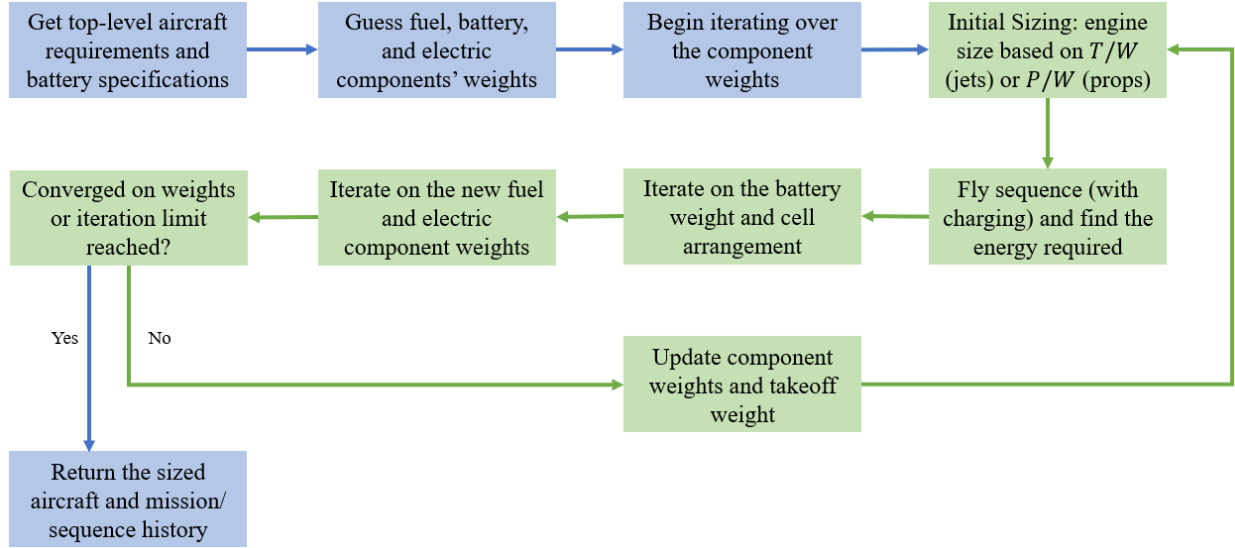
Fig. 12 Computational procedure for aircraft sizing.

the beginning of each mission, which is influenced by factors such as charging time and power. Cases with inadequate energy to follow the designated power management strategy are deemed infeasible, and no changes to operational conditions or power management strategies are made in such instances.

A. Problem Formulation

An example application, comprising the notional ERJ-175 and its corresponding hybrid electric aircraft (HEA) models, is provided to demonstrate the use of the developed technical approach. The problem formulation is organized based on the three-step approach established earlier, consisting of identifying the market, designing the aircraft, and simulating operations.

Step 1: Identify. The ERJ-175 was selected as the reference aircraft to represent the target regional jet market. A notional ERJ-175 model was created using publicly available data from the literature [31] and sized based on the top-level aircraft requirements (TLARs) and design mission profile of the reference aircraft. Table 2 displays the design mission profile obtained from Ref. [31]. The reserve mission comprises two components: a 100 nmi alternate and a 45-minute reserve flight. The 45-minute flight is estimated as an additional cruise segment with a 337 nmi distance flown at cruise speed, resulting in a total reserve mission range of 437 nmi, which is added to the design range.

The reference aircraft was sized using the in-house aircraft sizing tool, resulting in the creation of the baseline notional ERJ-175 model. During the sizing process, calibrations were performed on the climb and cruise lift-to-drag ratio and cruise thrust specific fuel consumption (TSFC) for the reference aircraft to align the baseline aircraft model's TOGW, OEW, and fuel burn after sizing with literature values. These calibration factors remain constant for all other sizing conditions. The resulting model is shown and compared to the actual values found in the literature for the ERJ-175 in Table 3. The results indicate percent errors less than around 2

Table 2 Design and Reserve Mission Profiles obtained from literature [31]

Payload [lb]	7800
Range [nmi]	1650
Cruise Altitude [ft]	35000
Cruise Speed [KTAS]	450
Reserve Distance (total) [nmi]	437

Table 3 Baseline aircraft model comparisons against the representative ERJ-175 from the literature.

	Reference aircraft	Baseline model	% Error
MTOW [lb]	82673	84050	1.67
OEW [lb]	47399	48161	1.61
Fuel weight [lb]	18075	18036	-0.22
Wing Loading	105.6	105.6	N/A
Thrust to Weight	0.3435	0.3435	N/A

Step 2: Design. The design process focused on parallel hybrid electric aircraft (HEA) models. Multiple HEA models were created for varying power management scenarios (power splits), battery technology levels (varying specific energy), and design range requirements. Specifically, the following variations were considered:
- Power splits: 5% takeoff, 10% takeoff, 15% takeoff, 5% takeoff and 5% climb, and 10% takeoff and 10% climb.
- Battery technology levels: 250 Wh/kg and 500 Wh/kg.
- Design range requirements: 1650 nmi (the original design range of the reference aircraft) and 1000 nmi (a reduced design range to serve the short haul market).

Because the varying power splits play a crucial role in the feasibility a benefit assessments, a special notation was established to differentiate the HEA sized for different power management strategies that were followed, as shown in Table 4. Note that power split refers to the maximum electric motor power as a percentage of the total shaft power required at sea level static takeoff conditions. The maximum power capability of the HEA system is sized for this condition, while the energy requirements is sized as a combination of battery power required at each point in flight and the duration of battery usage.

Table 4   HEA Notation

Notation	Power Split
HEA1	5% takeoff
HEA2	10% takeoff
HEA3	15% takeoff
HEA4	5% takeoff + 5% climb
HEA5	10% takeoff + 10% climb

Tables 5 and 6 show model comparisons for the original design range and the reduced design range respectively. The baseline aircraft is compared to the HEA configurations, which are described in Table 4. The tables listed in this section are representative for the battery with 0.25 kWh/kg specific energy. The cases for the 0.5 kWh/kg specific energy are listed in the Appendix.

The results of the sizing analysis show that while the HEA designs with takeoff hybridization (HEA 1, 2, and 3) show slight fuel burn benefits over their respective conventional baseline aircraft, a climb hybridization brings significant fuel burn penalties (HEA 4 and 5). Nevertheless, all HEA configurations were carried forward to the operational analysis to investigate the impact of operational metrics on fuel burn under varying design conditions.

Step 3: Operate. HEA operations were simulated on historical route sequences for all sized HEA, considering varying ground times that can affect the battery state of charge (SOC) at the beginning of each flight mission. The mission analysis block simulated the flight, determining the required fuel burn and final battery SOC. This iterative process continued until the fuel and takeoff gross weight values converged. Upon landing at the destination airport, the operational analysis block provided ground time information to the charging analysis block. The battery was charged at a given rate, varying between 150 kW/h (a moderate estimate for current technology) and 400 kW/h (state-of-the-art estimate), for the entire duration of the ground time, or until the battery SOC reached 100%, whichever came first. The new SOC served as the initial SOC for the next flight mission. The operational analysis block set the mission profile for the subsequent mission in the route sequence, and the process described in the previous steps was repeated for the new mission. This process continued until all missions in the sequence were simulated. The output of this process was a

Table 5   Model comparisons between the baseline conventional aircraft (notional ERJ-175), and the HEA configurations sized for 0.25 kWh/kg specific energy, 1650 nmi original design range.

	Original Range Baseline	HEA 1	HEA 2	HEA 3	HEA 4	HEA 5
MTOW	0% (84050 lb)	-0.87%	-1.75%	-2.58%	14.33%	33.66%
OEW	0% (48161 lb)	-1.53%	-3.06%	-4.53%	13.57%	31.88%
Fuel Burn	0% (18036 lb)	-0.92%	-1.87%	-2.75%	13.33%	31.25%

Table 6   Model comparisons between the representative ERJ175, the sized ERJ175, and its configurations for 0.25 kWh/kg specific energy, 1000 nmi range.

	Reduced Range Baseline	HEA 1	HEA 2	HEA 3	HEA 4	HEA 5
MTOW	0% (67370 lb)	-0.71%	-1.40%	-2.11%	11.33%	25.30%
OEW	0% (38603 lb)	-1.37%	-2.71%	-4.06%	10.59%	23.63%
Fuel Burn	0% (10913 lb)	-0.79%	-1.57%	-2.36%	10.06%	22.40%

detailed summary of the aircraft performance, including the mission history, fuel burn, and battery SOC as a function of time throughout the sequence.

In the operational analysis, all HEA models were operated using their original takeoff and climb power split strategies. It was observed that, in most cases, the actual TOGW of the HEA was less than the maximum takeoff weight for which the aircraft was sized. Due to the changing TOGW, the takeoff and climb thrust and power requirements also changed, while the power splits were maintained at relative values with respect to the total thrust and power requirements. Consequently, in some instances, there was surplus energy in the battery after completing the climb segment. For cases with leftover energy in the battery at the top of the climb, this energy was utilized during the cruise phase until the battery reached a 20% SOC. The results were then compared to the baseline conventional aircraft to evaluate the fuel reduction achieved by the HEA models.

The following sections provide a detailed description of the results of the analysis performed.

B. Sequence Analysis

The filtering of sequences from the BTS data [28] is based on flight distance and ground time between flights, because the flight distance of HEA is limited by the weight of the batteries, and ground time determines the charging time for the HEA before the next flight. For this study, the flight distance limit is chosen to be 800 nmi, and the ground time limit is chosen to be 50 min. However, there is a wide range of choices on how much battery power and fuel to carry for a flight. Thus, it is not required that all the flights meet the flight distance and ground time limits. Instead, within each sequence, a flight with a flight distance over 800 nmi and a flight with a ground time less than 50 minutes are allowed.

Table 7 is the sequence finally selected from [28] to run the aircraft model and the simulation model with. The Ground Time column in Table 7 represents the ground time at the origin airport before each flight. The first flight does

not have a ground time because the aircraft spends the night at the gate, providing sufficient time for charging. In this sequence, there is a medium-haul flight (MCI-SFO) and four short-haul flights (ORD-DTW, DTW-ORD, ORD-MCI and SFO-SBP), hence the model can be tested for both short-haul and medium-haul performance.

Table 7   Sequence Information

Routes	Distance (nmi)	Ground Time (min)
ORD-DTW	204.2	–
DTW-ORD	204.2	36
ORD-MCI	350.2	70
MCI-SFO	1302.6	116
SFO-SBP	165.1	57

Figure 13 reflects the sequence in Table 7 geographically. Furthermore, the original design range of 1650 nmi and the reduced design range of 1000 nmi are shown around the hub of the sequence, Chicago O'Hare International Airport (ORD). As shown by the original design range circle, the original design range-sized HEA have the range to service medium haul flights, and even any flight to the continental United States out of Chicago.
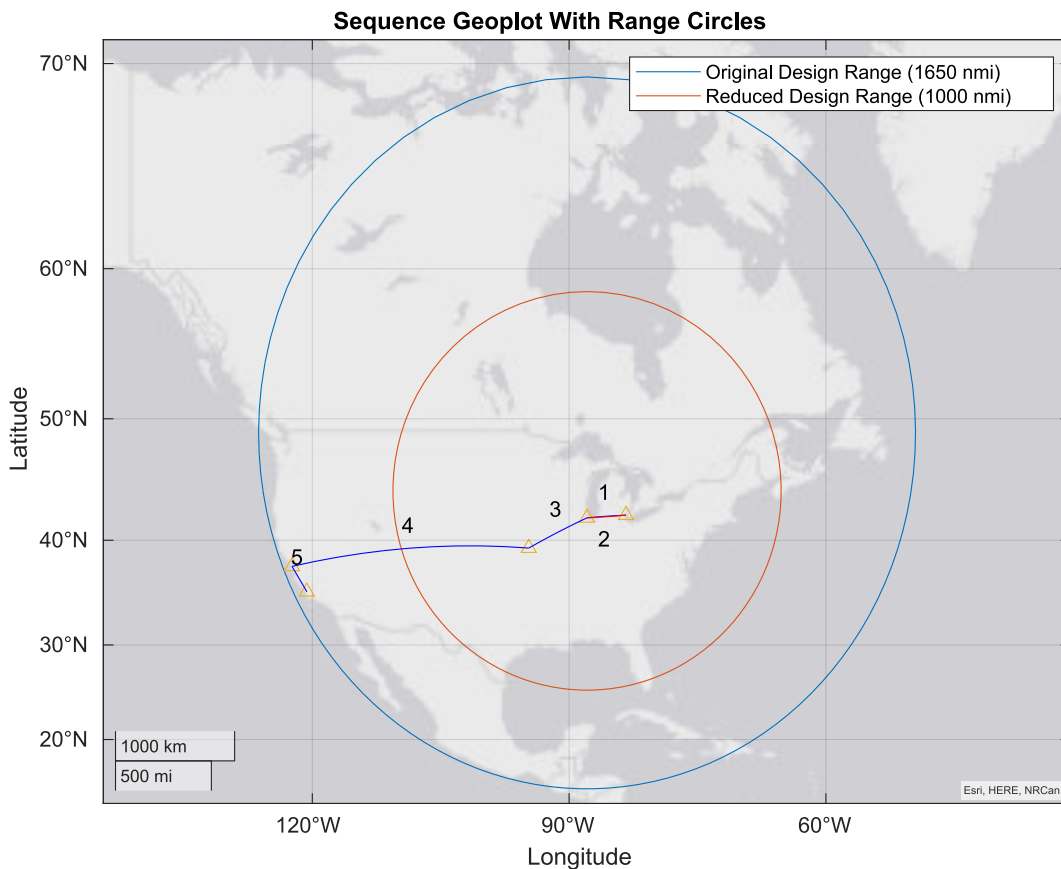

Fig. 13   Sequence GeoPlot

Figures 14 and 15 display the sequence in Table 7 in terms of both airport vs time (Greenwich Mean Time) and SOC (%) vs time (Greenwich Mean Time). Fig 14 shows the sequence modelled for all 5 HEA, with an airport charging rate

of 150 kW/h and a battery specific energy of 250 Wh/kg. Likewise, Fig 15 also shows the sequence modelled for all 5 HEA with a battery specific energy of 250 Wh/kg, though with an airport charging rate of 400 kW/h. The dashed line at 20% SOC represents the minimum SOC allowed for feasibility, as discharging the battery past that point could permanently damage the battery. Any plots with an SOC below 20% indicate that a flight, and consequently the entire sequence, is not feasible.

For a charging rate of 150 kW/h and a battery specific energy of 250 Wh/kg, the sequence is not feasible for HEA4 and HEA5. Both HEA, which have hybridized climb, fail to charge sufficiently for the next flight after completing the first flight in the sequence.

Meanwhile, maintaining a battery specific energy of 250 Wh/kg, but as seen in Fig 15, using an airport charging rate of 400 kW/h the overall feasibility of this sequence improves. The sequence is now feasible for all HEA options outside of HEA4. HEA4 now fails during the longest route of the sequence (MCI to SFO), and its infeasibility is not due to its SOC, as the initial SOC prior to the flight is 100% and never falls below 20%. This result requires further investigation and analysis to identify the cause of failure, which might be rooted in other operational requirements such as cruise speed.

Figures 16 through 24 show a sequence flight results for a flight between the San Francisco International Airport (SFO) and San Luis Obispo County Regional Airport (SBP). The plots include the comparison between the on-design and off-design mission profiles for altitude, distance flown, battery energy, electric motor power, total fuel burned, state of charge, true airspeed, thrust, and weight of the aircraft. As this was the last flight in that sequence, the battery was not fully charged, which is reflected in Fig 18 and 21 specifically. It is worth noting that the on-design mission is longer than the off-design mission; however, for the sake of comparison, only the off-design time portion is considered.

Comparing the on and off-design mission on Fig 16, it can be seen that the on-design altitude reaches almost 11 km, which is near the peak altitude for most commercial airlines. The off-design mission follows the altitude climb until it reaches the mission's altitude. Figure 17 shows the comparison in distance covered by the flight. Once again, the on-design aircraft covers more distance in less time to maximize the performance of the aircraft. Additionally, the aircraft's climb is longer than that one of the off-design.

In Fig 18 the comparison in leftover battery energy is shown. It is worth noting that the initial energies are different, but the trends are as follows: for the on-design mission, there is a consistent energy usage during the takeoff and climb segments, which drains the battery until cruise when the power is no longer used; as for the actual off-design mission, there is a 5% power split during the takeoff and climb segments. The off-design climb segment is shorter than its on-design counterpart, but the leftover battery energy is then used in the cruise segment to bring the battery's state of charge close to 20%. Figure 19 highlights that difference. The on-design electric motor power is not being used during the cruise segment, while the off-design mission uses the remaining potential of the battery. This difference is also shown in Fig 21, which shows the SOC comparison of the two missions.

Figure 22 shows similar results to the altitude comparison between the missions: once the target airspeed is reached at the end of the climb segment, it is maintained until the end of the cruise segment. The on-design mission airspeed is greater than that of the off-design. The trends of the thrust are shown in Fig 23. The two missions follow the same pattern of thrust - with less amount of force needed as the climb segment continues. Then, a constant values is reached and maintained until the end of the cruise segment. Once again, the thrust of the off-design mission is smaller than that of the on-design.

Finally, Fig 24 shows the weight of the aircraft for the two missions. While the trends may appear similar at first glance, the on-design mission loses more weight over time, as it burns a significantly larger amount of fuel, as seen in Fig 20..

C. Fuel Burn Predictions and Sensitivity Studies

Simulations are run with different charge rates at airports, specific energy of batteries, and aircraft sizes. The combination of a 150 kW/h charge rate and 0.25 kWh/kg battery specific energy is the most realistic and conservative case, whereas the combination of a 400 kW/h charge rate and 0.5 kWh/kg battery specific energy is the most ambitious case.

A conventional aircraft resized for a 1000 nmi range is also included for comparison to assess the fuel burn between HEA and conventional aircraft with similar range limits and to verify that introducing HEA is more beneficial than redesigning downsized conventional aircraft.

Tables 8 and 9 are the simulation results of take-off gross weight in kg and fuel burn in kg with 150 kW/h charge rate and 0.25 kWh/kg specific energy of the battery for aircraft at the design range. The "baseline" refers to a conventional
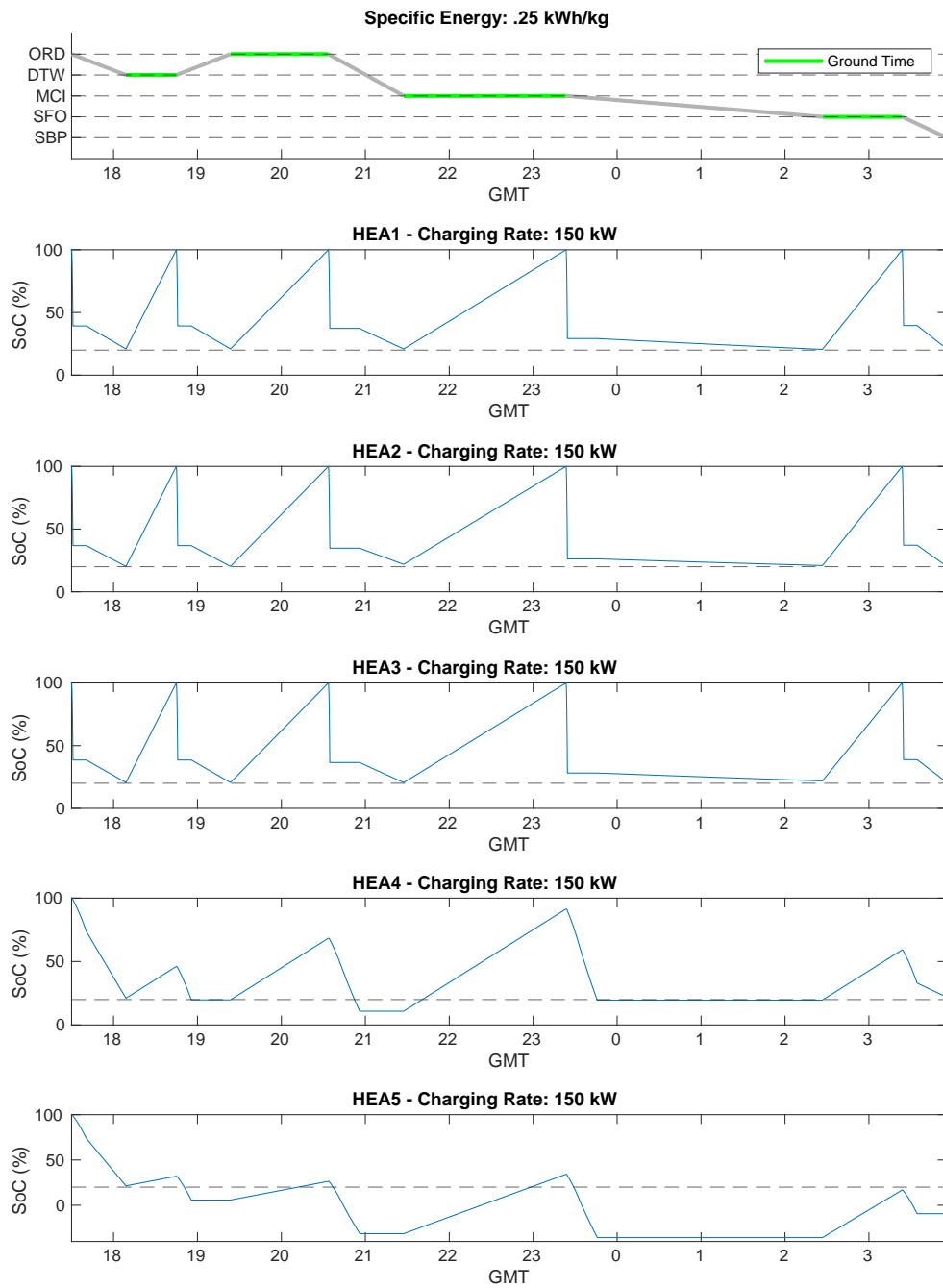
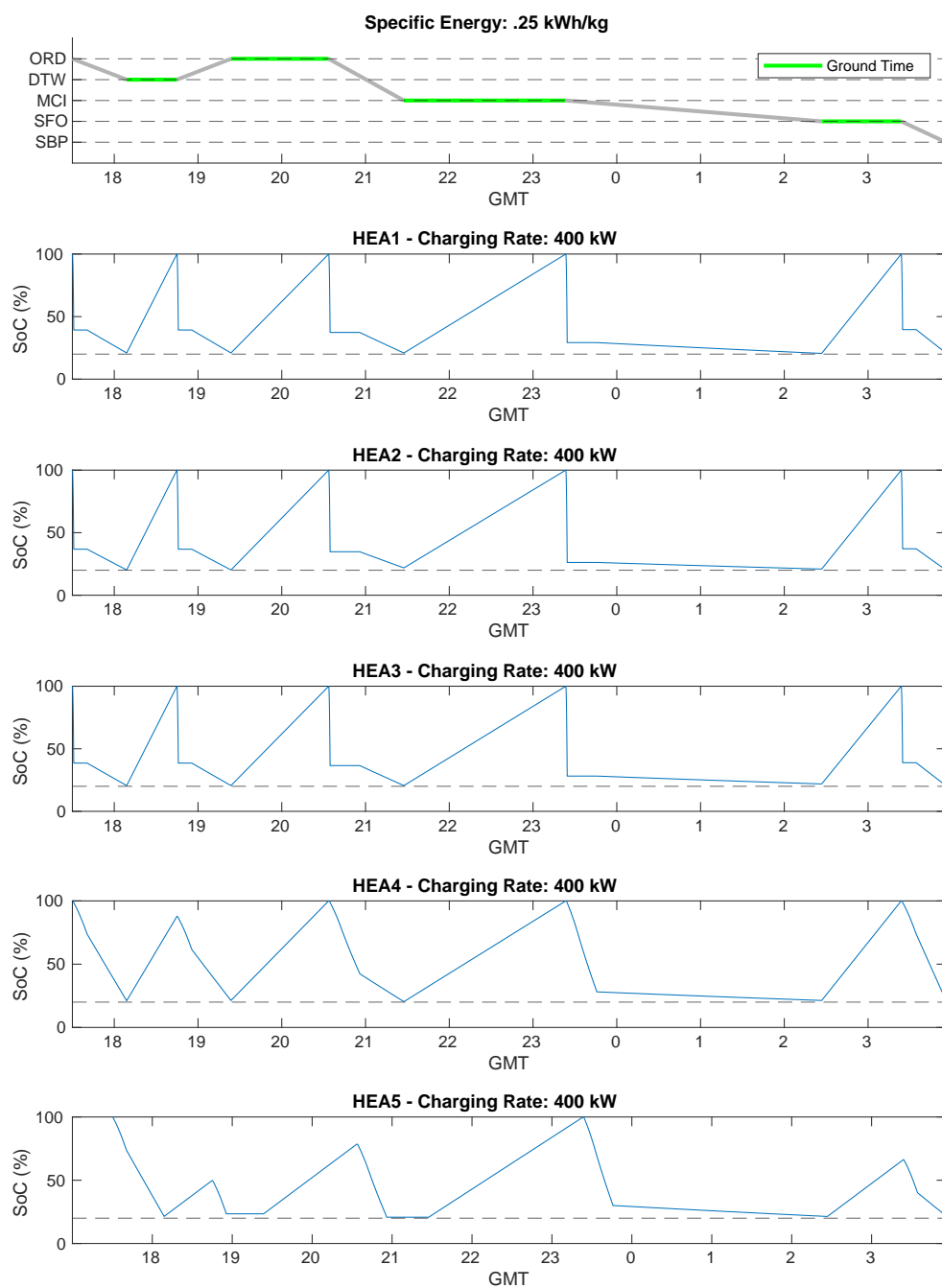**Fig. 14 Sequence SOC history with a battery charging rate of 150 kW/h.**

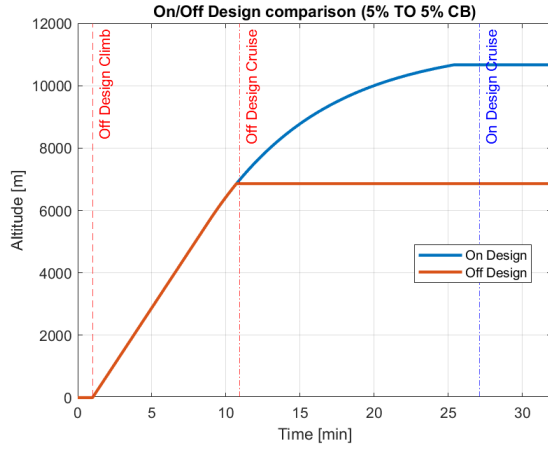**Fig. 15 Sequence SOC history with a battery charging rate of 400 kW/h.**

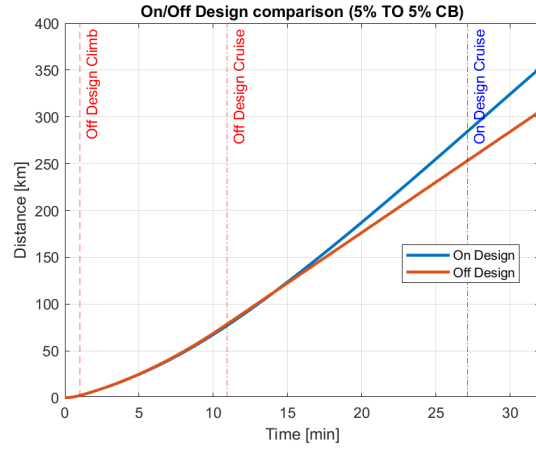**Fig. 16   Altitude comparison for HEA 4.**
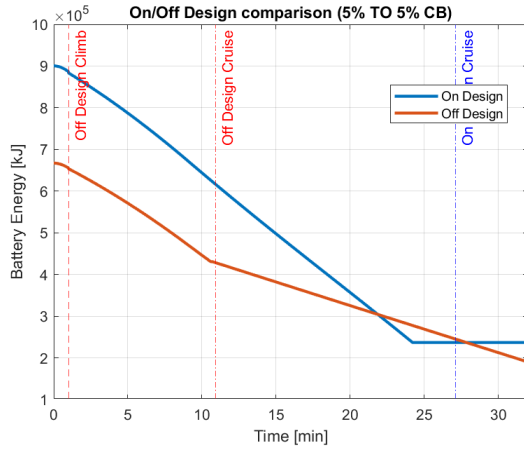

Fig. 17   Distance comparison for HEA 4.

Fig. 18   Battery energy comparison for HEA 4. (initial SOC for the off-design case is of 74.1%, whereas the on-design case starts with a 100% SOC).

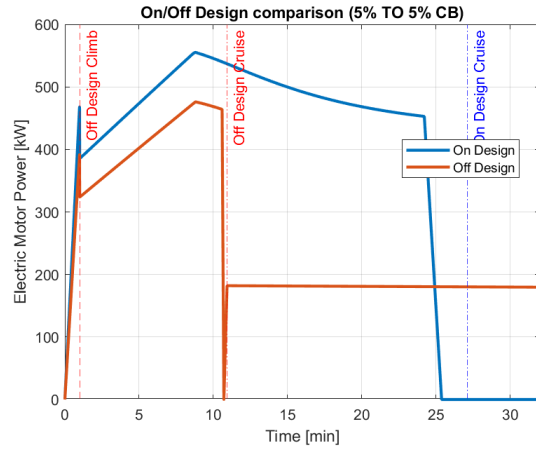**Fig. 19   Electric motor power comparison for HEA 4.**
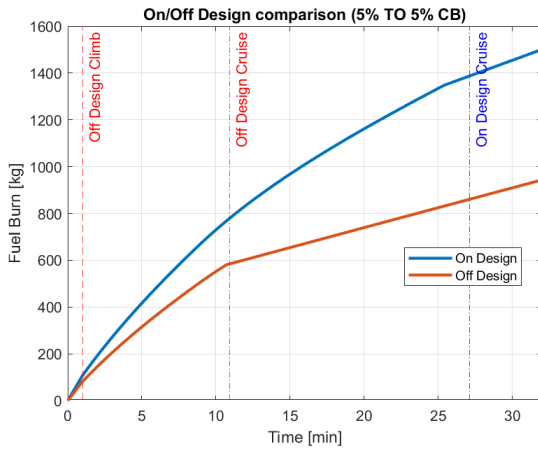.
.

Fig. 20   Fuel burn comparison for HEA 4.
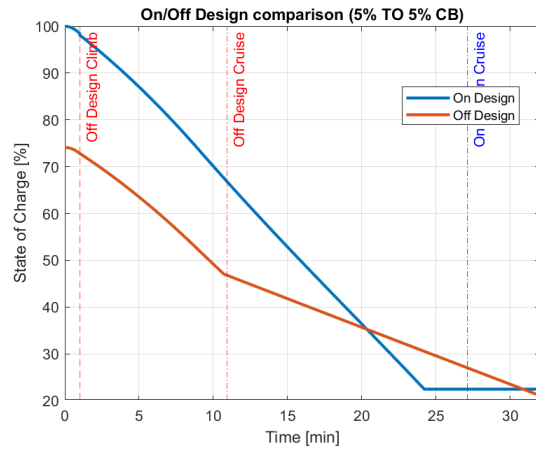.
.

Fig. 21   State of charge comparison for HEA 4. (note the initial SOC 74.1% for off-design vs. 100% for on-design).
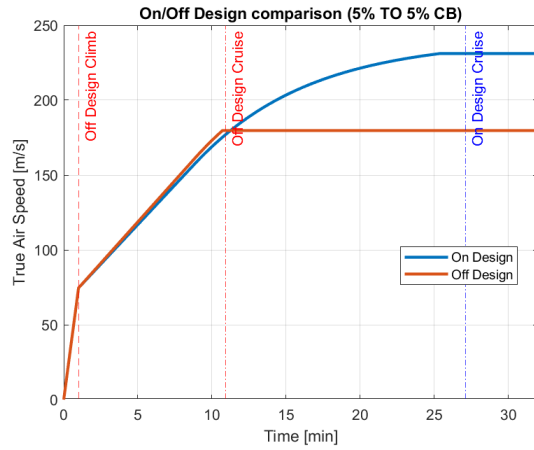
22

Fig. 22   True airspeed comparison for HEA 4.
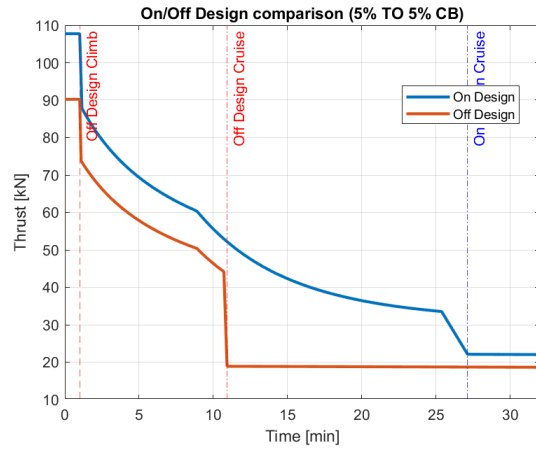

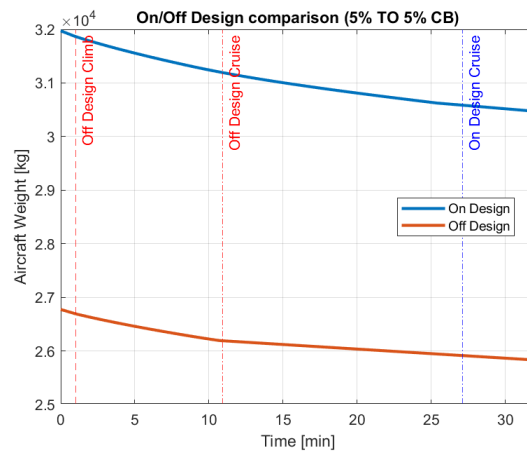**Fig. 23   Thrust comparison for HEA 4.**

Fig. 24   Aircraft weight comparison for HEA 4.

configuration, where no battery is carried and the flight is only powered by fuel consumption. NF signifies that the design was Not Feasible due to the battery discharging below 20% or TOGW being larger than the MTOW. Thus, the designs are marked as infeasible.

Table 8   Take Off Gross Weight (kg) (150 kW/h charge rate, 0.25 kWh/kg specific energy, design range)

Routes	Baseline	HEA 1	HEA 4	HEA 2	HEA 5	HEA 3
ORD-DTW	30287.00	29956.96	34678.99	29625.35	40614.97	29309.29
DTW-ORD	30287.00	29956.96	NF	29625.35	NF	29309.29
ORD-MCI	31287.00	30921.38	NF	30580.23	NF	30255.06
MCI-SFO	35287.00	34921.38	NF	34580.23	NF	34255.06
SFO-SBP	30134.29	29800.19	34538.48	29470.27	NF	29155.80

Table 9   Fuel Burn (kg) (150 kW/h charge rate, 0.25 kWh/kg specific energy, design range)

Routes	Baseline	HEA 1	HEA 4	HEA 2	HEA 5	HEA 3
ORD-DTW	1255.35	1236.93	1350.87	1218.47	1480.42	1200.62
DTW-ORD	1255.35	1236.77	NF	1218.30	NF	1200.46
ORD-MCI	2116.25	2085.79	NF	2057.23	NF	2029.67
MCI-SFO	5817.82	5751.55	NF	5689.55	NF	5630.19
SFO-SBP	1115.32	1098.05	1229.80	1081.11	NF	1064.73

Tables 9 and 8 with absolute values are provided for reference, and the change in percentage can be found below.

Table 10   TOGW Change (%) (150 kW/h charge rate, 0.25 kWh/kg specific energy, design range)

Routes	Baseline	HEA 1	HEA 4	HEA 2	HEA 5	HEA 3
ORD-DTW	0 (30287.00)	-1.10%	12.66%	-2.23%	25.43%	-3.34%
DTW-ORD	0 (30287.00)	-1.10%	NF	-2.23%	NF	-3.34%
ORD-MCI	0 (31287.00)	-1.18%	NF	-2.31%	NF	-3.41%
MCI-SFO	0 (35287.00)	-1.05%	NF	-2.04%	NF	-3.01%
SFO-SBP	0 (30134.29)	-1.12%	12.75%	-2.25%	NF	-3.36%

Tables 10 and 11 indicate that as the TOGW decreases, fuel burn correspondingly decreases, whereas an increase in TOGW results in increased fuel burn. Thus the following discussion and analysis will focus on fuel burn, as fuel burn and TOGW exhibit parallel trends. Table 11 shows that for HEA1, 2, and 3, where only takeoff is hybridized, there is a considerable reduction in fuel burn compared to the baseline, and the fuel savings increase with the hybridization level. For HEA4 and 5, where both takeoff and climb are hybridized, most flights in the sequence are not feasible, and the only three feasible flights result in increased fuel burn.

As this study includes a notional ERJ-175 model with the original design range and an aircraft model with a reduced range of 1000 nmi, the following discussion will address these two cases separately before comparing them at the end.

1. Fuel Burn Change in Aircraft Sized for the Original Design Range Mission

Tables 11 to 14 present the fuel burn change in percentage for all operation cases in the design range of the ERJ-175 aircraft.

The results in Tables 11 to 14 demonstrate that for HEA 1, 2, and 3, all flights are feasible with fuel savings ranging from 1.49% to 5.20%. Additionally, a higher level of hybridization corresponds to a greater decrease in fuel burn.

24

Table 11　Fuel Burn Change (%) (150 kW/h charge rate, 0.25 kWh/kg specific energy, design range)

Routes	Baseline	HEA 1	HEA 4	HEA 2	HEA 5	HEA 3
ORD-DTW	0 (1255.35)	-1.49%	7.07%	-3.03%	15.20%	-4.56%
DTW-ORD	0 (1255.35)	-1.50%	NF	-3.04%	NF	-4.57%
ORD-MCI	0 (2116.25)	-1.46%	NF	-2.87%	NF	-4.26%
MCI-SFO	0 (5817.82)	-1.15%	NF	-2.25%	NF	-3.33%
SFO-SBP	0 (1115.32)	-1.57%	9.31%	-3.16%	NF	-4.75%

Table 12　Fuel Burn Change (%) (150 kW/h charge rate, 0.5 kWh/kg specific energy, design range)

Routes	Baseline	HEA 1	HEA 4	HEA 2	HEA 5	HEA 3
ORD-DTW	0 (1255.35)	-1.64%	-0.80%	-3.32%	-1.68%	-5.01%
DTW-ORD	0 (1255.35)	-1.65%	2.78%	-3.33%	NF	-5.02%
ORD-MCI	0 (2116.25)	-1.61%	NF	-3.16%	NF	-4.71%
MCI-SFO	0 (5817.82)	-1.28%	3.39%	-2.51%	NF	-3.72%
SFO-SBP	0 (1115.32)	-1.72%	1.33%	-3.45%	NF	-5.20%

Table 13　Fuel Burn Change (%) (400 kW/h charge rate, 0.25 kWh/kg specific energy, design range)

Routes	Baseline	HEA 1	HEA 4	HEA 2	HEA 5	HEA 3
ORD-DTW	0 (1255.35)	-1.49%	7.07%	-3.03%	15.20%	-4.56%
DTW-ORD	0 (1255.35)	-1.50%	7.83%	-3.04%	21.44%	-4.57%
ORD-MCI	0 (2116.25)	-1.46%	9.14%	-2.87%	20.75%	-4.26%
MCI-SFO	0 (5817.82)	-1.15%	NF	-2.25%	29.03%	-3.33%
SFO-SBP	0 (1115.32)	-1.57%	6.29%	-3.16%	18.56%	-4.75%

Table 14　Fuel Burn Change (%) (400 kW/h charge rate, 0.5 kWh/kg specific energy, design range)

Routes	Baseline	HEA 1	HEA 4	HEA 2	HEA 5	HEA 3
ORD-DTW	0 (1255.35)	-1.64%	-0.80%	-3.32%	-1.68%	-5.01%
DTW-ORD	0 (1255.35)	-1.65%	-0.40%	-3.33%	4.95%	-5.02%
ORD-MCI	0 (2116.25)	-1.61%	1.41%	-3.16%	4.31%	-4.71%
MCI-SFO	0 (5817.82)	-1.28%	3.29%	-2.51%	NF	-3.72%
SFO-SBP	0 (1115.32)	-1.72%	-1.65%	-3.45%	0.95%	-5.20%

Comparing Tables 11 and 12, and Tables 13 and 14, it is apparent that advancements in battery specific energy enable some flights with HEA 4 and 5, in which both takeoff and climb are hybridized. The remaining infeasible flights are medium-haul flights that may require a higher hybridization level. However, most flights utilizing HEA 4 and 5 do not result in fuel savings. Furthermore, increased specific energy can bring more fuel savings for HEA 1, 2, and 3.

Comparing Tables 11 and 13, and Tables 12 and 14, it becomes clear that advancements in airport charge rate can enable some flights with HEA 4 and 5. For flights with sufficient ground time to charge to the required final SOC, the charge rate does not affect fuel burn change. However, in cases where ground time is short or final SOC is high, improvements in charge rate can effectively enable flights and decrease fuel burn rise, primarily for HEA 4 and 5.

2. Fuel Burn Change in Aircraft Sized for the Reduced Design Range Mission

Results in Tables 15 to 18 indicate that for HEA 1, 2, and 3, most flights are feasible with fuel savings ranging from 1.30% to 4.52%. Consistent with previous observations, a higher level of hybridization leads to a greater decrease in fuel burn. However, all simulation results show that the fourth flight "MCI-SFO" is infeasible, which is logical since all aircraft have a range limit at 1000 nmi, and TOGW would exceed the limit if the aircraft were to fly a distance of about 1300 nmi.

Comparing Tables 15 and 16, and Tables 17 and 18, it is evident that advancements in battery specific energy cannot enable any infeasible flights with HEA 4 and 5. However, the advancement in battery technology effectively reduces fuel burn for all HEA configurations, and some flights with HEA 4 and 5 end up with decreased fuel burn.

Comparing Tables 15 and 17, and Tables 16 and 18, it is apparent that advancements in airport charge rate can enable some flights with HEA 5. Similar to the previous observation, for flights with sufficient ground time to charge to the required final SOC, the charge rate does not affect the fuel burn change. However, in cases where ground time is short or final SOC is high, improvements in charge rate can effectively enable flights and decrease fuel burn rise for HEA5.

Table 15   Fuel Burn Change (%) (150 kW/h charge rate, 0.25 kWh/kg specific energy, 1000 nmi range)

Routes	Baseline	HEA 1	HEA 4	HEA 2	HEA 5	HEA 3
ORD-DTW	0 (1067.47)	-1.30%	4.80%	-2.63%	10.05%	-3.99%
DTW-ORD	0 (1067.47)	-1.31%	7.98%	-2.64%	NF	-4.00%
ORD-MCI	0 (1794.01)	-1.19%	7.44%	-2.39%	NF	-3.62%
MCI-SFO	0 (5861.30)	NF	NF	NF	NF	NF
SFO-SBP	0 (947.61)	-1.37%	6.17%	-2.74%	NF	-4.16%

Table 16   Fuel Burn Change (%) (150 kW/h charge rate, 0.5 kWh/kg specific energy, 1000 nmi range)

Routes	Baseline	HEA 1	HEA 4	HEA 2	HEA 5	HEA 3
ORD-DTW	0 (1067.47)	-1.42%	-1.62%	-2.87%	-3.53%	-4.34%
DTW-ORD	0 (1067.47)	-1.43%	1.56%	-2.88%	NF	-4.36%
ORD-MCI	0 (1794.01)	-1.31%	1.25%	-2.39%	NF	-3.62%
MCI-SFO	0 (5861.30)	NF	NF	NF	NF	NF
SFO-SBP	0 (947.61)	-1.48%	-0.46%	-2.99%	NF	-4.52%

Table 17 Fuel Burn Change (%) (400 kW/h charge rate, 0.25 kWh/kg specific energy, 1000 nmi range)

Routes	Baseline	HEA 1	HEA 4	HEA 2	HEA 5	HEA 3
ORD-DTW	0 (1067.47)	-1.30%	4.80%	-2.63%	10.05%	-3.99%
DTW-ORD	0 (1067.47)	-1.31%	4.78%	-2.64%	15.11%	-4.00%
ORD-MCI	0 (1794.01)	-1.19%	6.92%	-2.39%	14.88%	-3.62%
MCI-SFO	0 (5861.30)	NF	NF	NF	NF	NF
SFO-SBP	0 (947.61)	-1.37%	4.11%	-2.74%	11.48%	-4.16%

Table 18 Fuel Burn Change (%) (400 kW/h charge rate, 0.5 kWh/kg specific energy, 1000 nmi range)

Routes	Baseline	HEA 1	HEA 4	HEA 2	HEA 5	HEA 3
ORD-DTW	0 (1067.47)	-1.42%	-1.62%	-2.87%	-3.53%	-4.34%
DTW-ORD	0 (1067.47)	-1.43%	-1.63%	-2.88%	1.68%	-4.36%
ORD-MCI	0 (1794.01)	-1.31%	0.68%	-2.63%	1.35%	-3.98%
MCI-SFO	0 (5861.30)	NF	NF	NF	NF	NF
SFO-SBP	0 (947.61)	-1.49%	-2.45%	-2.99%	-3.41%	-4.52%

3. Comparing Aircraft with Different Ranges

Summarizing the results from Tables 11 to 18, it is clear that for all feasible cases, HEA 1, 2, and 3 result in fuel burn reductions at different levels. There is still considerable fuel saving when comparing HEA with down-sized conventional aircraft. The fuel burn benefits for down-sized aircraft models are lower, which is expected since a lower range conventional aircraft is more fuel-efficient, as observed from the baseline fuel burn results.

Focusing on HEA 4 and 5, some infeasible cases with the original design range become feasible with a lower range limit. However, the lower range limit restricts the aircraft from flying any flights beyond that range. Additionally, it can be concluded that higher specific energy of batteries leads to increased fuel savings. Starting with the same baseline fuel burn, a 0.25 kWh/kg increase in battery specific energy results in an increase in fuel savings ranging from 0.15% to 0.05% for the 5% takeoff, 10% takeoff, and 15% takeoff HEA. The increase in fuel burn for cases where both takeoff and climb are hybridized can also be mitigated.

4. In-Depth Sensitivity Analysis

Figure 25 is created for HEA where only takeoff is hybridized, with a 150 kW/h charge rate and 0.25 kWh/kg specific energy. It can be observed that fuel savings for longer flight missions decrease at all hybridization levels, with R^2 values greater than 0.97. Figure 25 also shows that fuel savings approximately increase linearly with hybridization level. To verify this observation, Fig 26 is created. By investigating the average fuel savings that HEA at different hybridization levels bring to the entire sequence, the linear growth trend is confirmed as R^2 is equal to 1.

To investigate the influence of battery specific energy on fuel savings, Fig 27 is generated. Comparing the three pairs of adjacent trending lines, it is clear that higher specific energy results in higher fuel savings. Combining Fig 27, Tables 11 and 12, it can be observed that the fuel burn benefit from battery specific energy is approximately constant for the same HEA configuration. Furthermore, with a 5% takeoff HEA, the increase in specific energy raises fuel savings by approximately 0.15%; the growth in fuel burn savings for a 10% takeoff HEA is about 0.30%; and similarly, the advancement of battery specific energy increases fuel burn savings for a 15% takeoff HEA by approximately 0.45%. Consequently, the fuel burn benefit from battery specific energy increases linearly with hybridization level.

Tables 19 through 21 compare the percent difference in thrust between different configurations, charging levels, and specific energies. Similar to the fuel burn percentage comparison, it can be seen that the charging rate has little effect on thrust changes, even though some missions become feasible due to the battery having enough charge for the next flight. As higher fuel burn savings are observed for designs with higher battery specific energy, these designs also require slightly less thrust. Comparing Tables 19 and 20, it can be seen that HEA 4 and HEA 5 configurations exhibit significant thrust reductions between the feasible missions. Moreover, the higher specific energy designs use about the
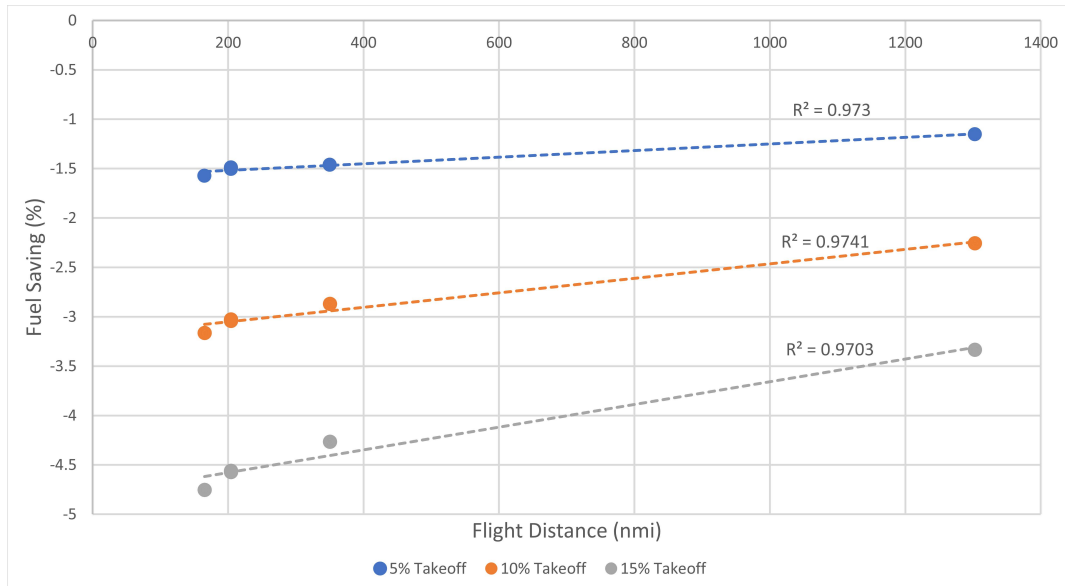
Fig. 25   Fuel Saving Comparison with Flight Distance (150 kW/h Charge Rate, 0.25 kWh/kg Specific Energy)
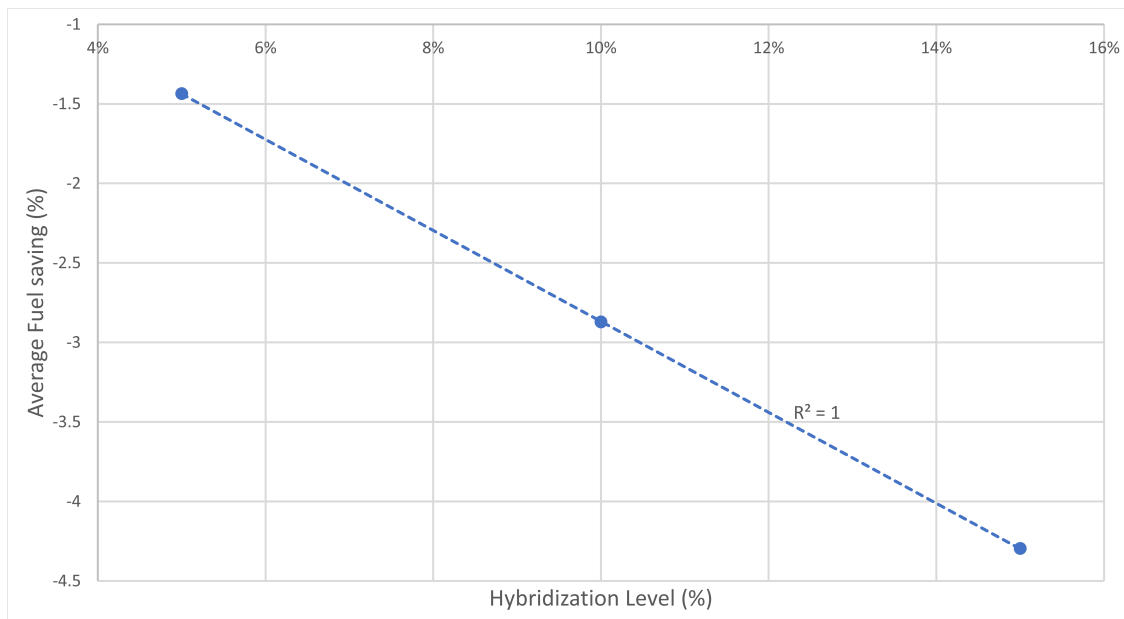

Fig. 26   Fuel Saving Comparison with Hybridization Level (150 kW/h Charge Rate, 0.25 kWh/kg Specific Energy)
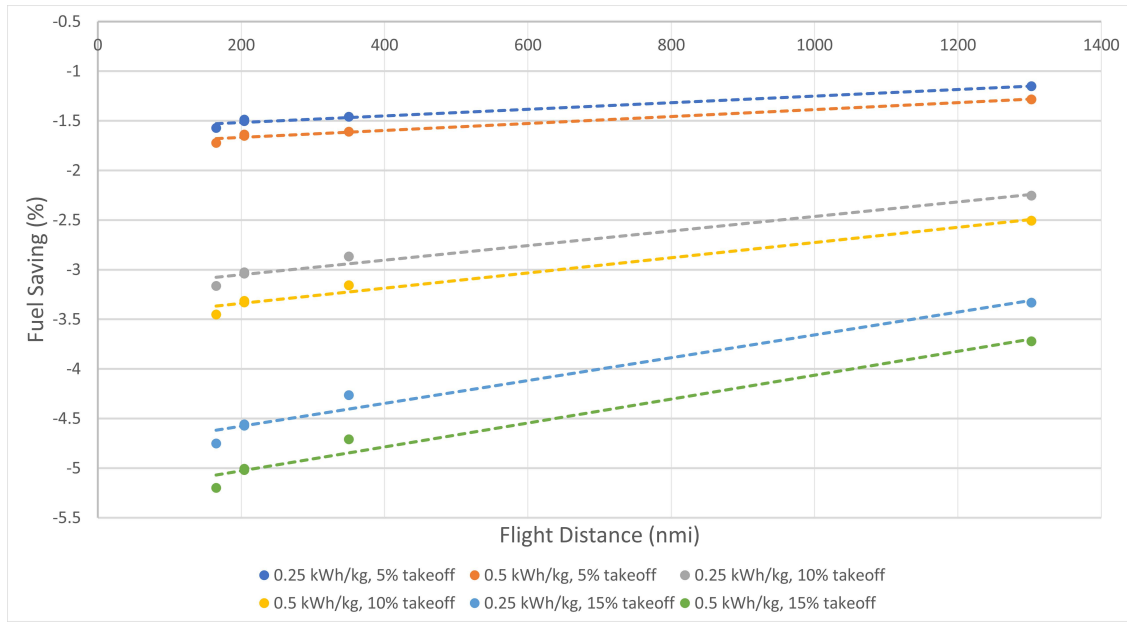
Fig. 27   Fuel Saving Comparison with Specific Energy (150 kW/h Charge Rate)

same amount or less thrust than conventional aircraft.

Table 19   Thrust at sea level Change (%) (150 kW/h charge rate, 0.25 kWh/kg specific energy, design range)

Routes	Baseline	HEA 1	HEA 4	HEA 2	HEA 5	HEA 3
ORD-DTW	0 (10404.25)	-6.04%	8.89%	-11.97%	20.69%	-17.74%
DTW-ORD	0 (10404.25)	-6.04%	NF	-11.97%	NF	-17.74%
ORD-MCI	0 (10747.78)	-6.11%	NF	-12.03%	NF	-17.80%
MCI-SFO	0 (12121.86)	-5.98%	NF	-11.80%	NF	-17.49%
SFO-SBP	0 (10351.79)	-6.05%	8.88%	-11.98%	NF	-17.76%

Table 20   Thurst at seal level Change (%) (150 kW/h charge rate, 0.5 kWh/kg specific energy, design range)

Routes	Baseline	HEA 1	HEA 4	HEA 2	HEA 5	HEA 3
ORD-DTW	0 (10404.25)	-6.17%	0.28%	-12.21%	0.77%	-18.09%
DTW-ORD	0 (10404.25)	-6.17%	0.38%	-12.21%	NF	-18.09%
ORD-MCI	0 (10747.78)	-6.25%	NF	-12.28%	NF	-18.15%
MCI-SFO	0 (12121.86)	-6.11%	-0.38%	-12.02%	NF	-17.79%
SFO-SBP	0 (10351.79)	-6.19%	0.38%	-12.23%	NF	-18.11%

Table 21   Thurst at sea level Change (%) (400 kW/h charge rate, 0.5 kWh/kg specific energy, design range)

Routes	Baseline	HEA 1	HEA 4	HEA 2	HEA 5	HEA 3
ORD-DTW	0 (10404.25)	-6.17%	0.28%	-12.21%	0.78%	-18.09%
DTW-ORD	0 (10404.25)	-6.17%	0.28%	-12.21%	0.10%	-18.09%
ORD-MCI	0 (10747.78)	-6.25%	0.11%	-12.28%	0.65%	-18.15%
MCI-SFO	0 (12121.86)	-6.11%	-0.47%	-12.02%	NF	-17.79%
SFO-SBP	0 (10351.79)	-6.19%	0.26%	-12.23%	0.91%	-18.11%

V. Conclusion and Future Work

This study presents strong evidence supporting the integration of hybrid electric aircraft (HEA) into the existing aviation network, given the availability of necessary charging infrastructure and power supplies. By using current aircraft turnaround times at the gate (i.e., ground turn times), it is possible to charge the aircraft without disrupting established flight schedules, allowing HEA to not only compete with conventional aircraft but also potentially replace them seamlessly in the future.

The primary goal of this paper was to investigate the feasibility of HEA within the context of airline operations, by analyzing aircraft design, battery sizing, and operational aspects under one comprehensive framework. This preliminary work successfully accomplished these goals by demonstrating that operating at different levels of hybridization can achieve 1-5% fuel savings compared to conventional aircraft, contributing to energy efficiency and environmental sustainability goals. When compared to downsized conventional aircraft with similar range limitations as HEA, the latter still offers considerable fuel savings, strengthening the argument for adopting HEA in the future.

An important conclusion to highlight is that when the HEA was compared against the conventional baseline, considering only the design mission (whether for the original design range or the reduced design range), the fuel burn benefits were not as pronounced. The true advantage of HEA came from operating them on shorter range missions, which represents the existing routes that airlines operate the representative aircraft at. This implies that the HEA may prove beneficial for regional airlines, where short-haul flights are the majority of their flights. It should be noted that some HEA configurations were unable to successfully complete certain mission legs, resulting in infeasible designs. However, the aircraft and flight operations can be further optimized, and this paper represents only a first step in the analysis.

Some benefits that electrified aircraft can offer are not fully represented in the current model. For instance, previous studies (such as Ref. [32]) have demonstrated that the takeoff power shaving of the gas turbine engine, combined with the electric motor boost, can lead to more efficient engine operation during the cruise segment, potentially resulting in additional fuel burn savings. This aspect was not considered in the present models but is part of the planned future work. Moreover, only constant power splits were investigated within each segment, while previous work by Cinar et al. [17] has shown that a more optimized varying power split strategy can yield further benefits. Despite these limitations, the results from this preliminary, first-order analysis are indeed promising.

Furthermore, advancements in battery technology could result in even greater improvements for HEA. Higher specific energy batteries could increase fuel savings and enhance overall HEA performance, while faster charging could improve the potential of sequences with shorter ground times. Continued advancements in battery technologies will be crucial for the successful implementation of HEA in the future.

Building upon the findings of this study, several next steps in research can be taken to better understand the advantages and limitations of HEA. A crucial next step is to explore a broader range of HEA configurations, refining the understanding of performance and fuel savings by changing the power splits for different segments based on the sized aircraft available power. Additionally, considering a wider variety of flight distances can help to size the aircraft accordingly and identify optimal flight distances for maximizing fuel savings at each level of hybridization.

Additionally, a wider variety of flight distances can be considered to size the aircraft accordingly. For each level of hybridization, it would be beneficial to identify the optimal flight distance with maximized fuel savings. Conversely, for different distances, the optimal hybridization level can be calculated to achieve maximum fuel savings. These simulations would allow to find the optimal design configuration for future HEA missions.

Another potential research direction involves analyzing a broader range of ground times and flight distances to determine the optimal use of HEA, accounting for different charging and refueling operations. This approach could shed light on logistical challenges during turnaround times at airports.

Finally, future work should aim to co-optimize aircraft design and operations by applying tail assignment and fleet assignment models to a small network serviced by HEA, simulating realistic airline decision-making processes regarding their network and operations. This could potentially magnify the 1-5% fuel savings, because the fleet and tail assignment optimization models would have a network-wide perspective on which routes to optimized (in terms of aircraft type and specific aircraft tail). In fact, previous work have already shown that the networks of NLC airlines (e.g., United Airlines) could be re-optimized to be more sustainable [33], and this was *without* consideration of advanced airframe and powertrains such as HEA. With HEA, such benefits could be much greater. In short, this approach would consider not only the technical aspects of HEA but also the strategies for navigating and managing routes, ensuring a more comprehensive understanding of the potential for HEA adoption in the aviation industry.

Acknowledgments

Appendix

A. SOC History Plots For Higher Technology Levels

Figures 28 and 29 show the airport and SOC history for all 5 original design range HEA with a battery specific energy of 500 Wh/kg for charging rates of 150 kW/h and 400 kW/h, respectively.
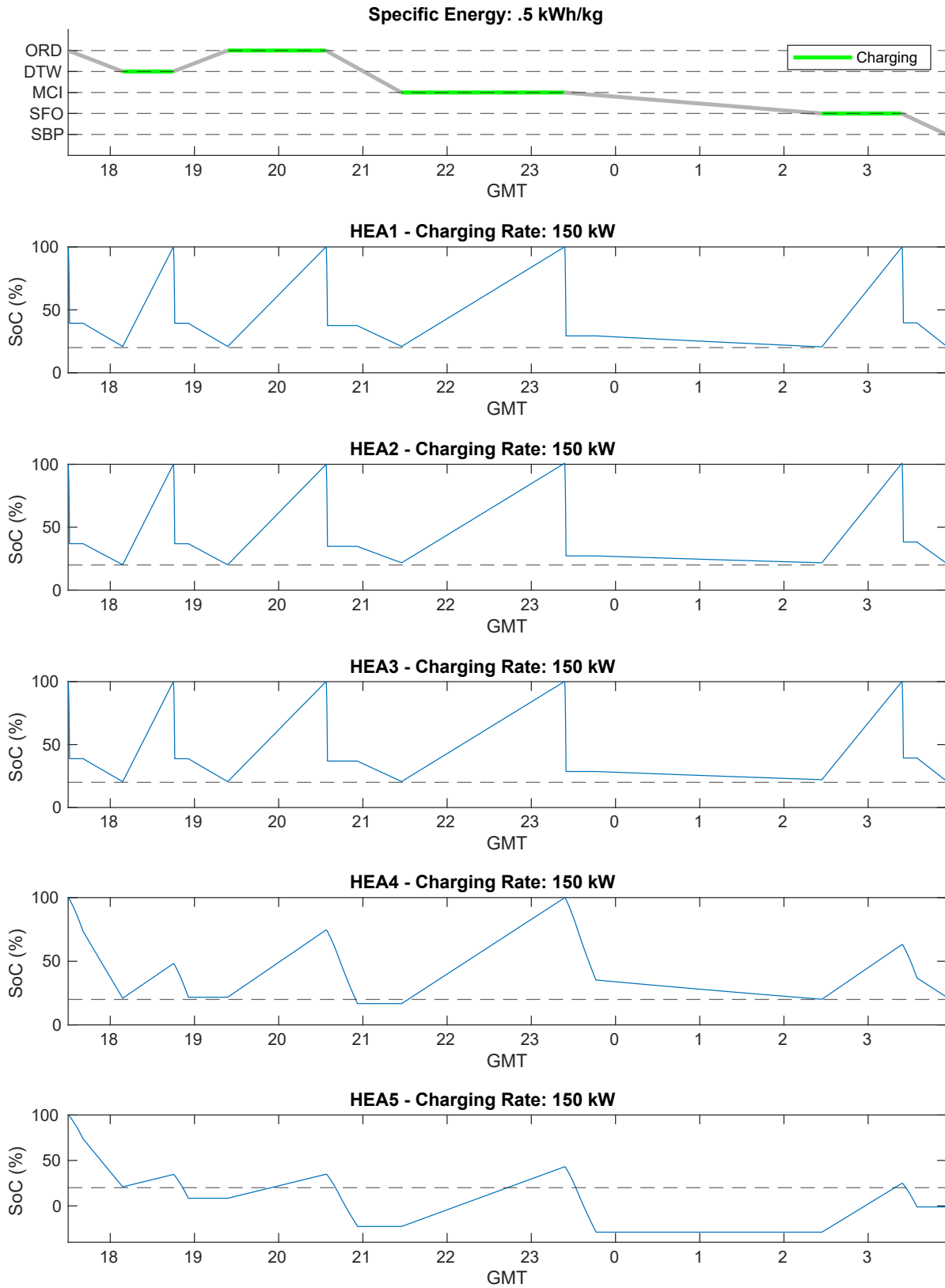
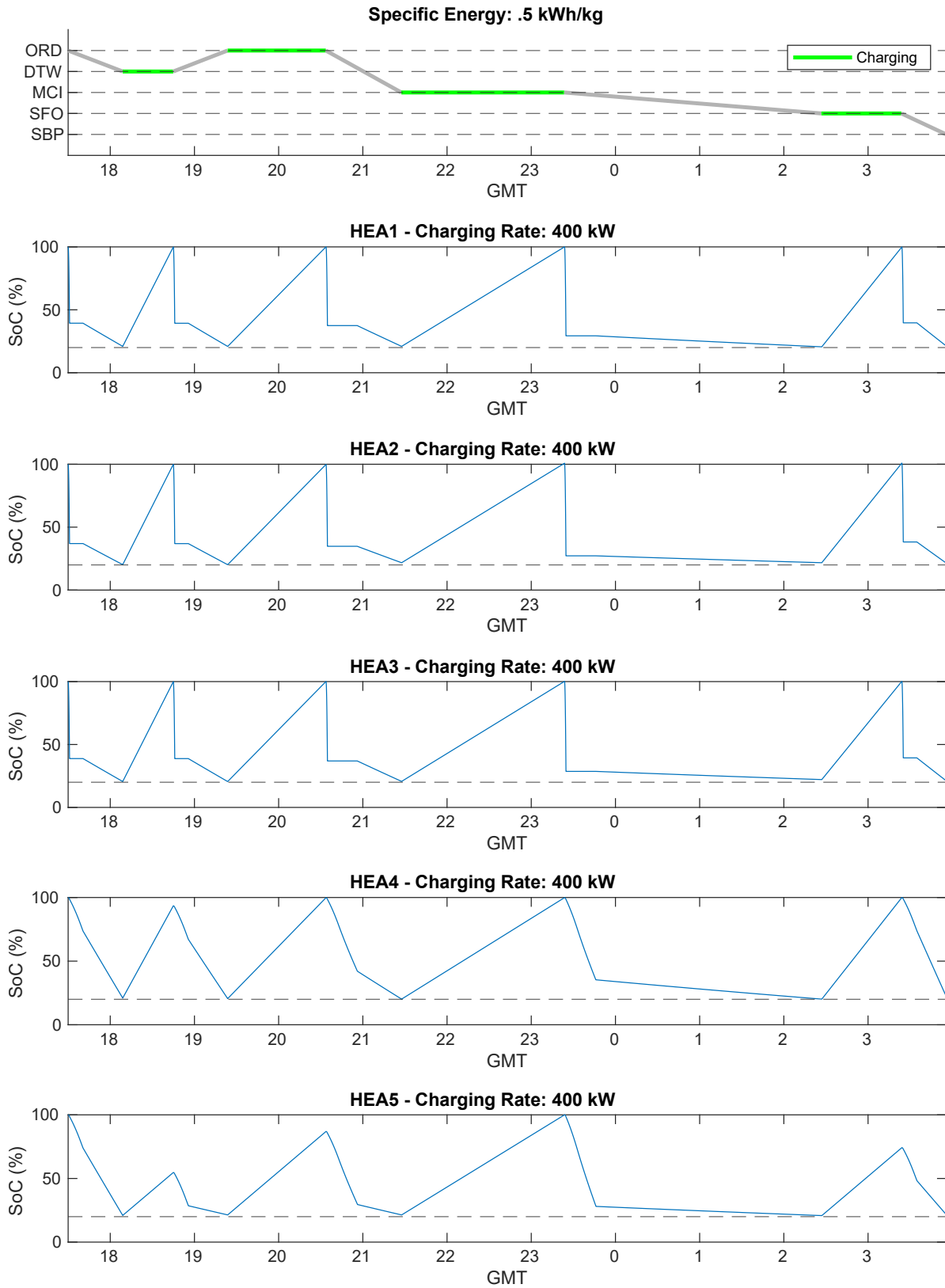**Fig. 28 Sequence SOC History - Charging Rate 150 kW/h**

Fig. 29   Sequence SOC History - Charging Rate 400 kW/h

B. Model Comparisons for 0.5 kWh/kg specific energy

Tables 22 and 23 compare the models for the original design range and the reduced design range, respectively, with a specific battery energy of 0.5 kWh/kg.

Table 22 Model comparisons between the representative ERJ175, the sized ERJ175, and its configurations for 0.5 kWh/kg specific energy, design range.

	ERJ175	Sized ERJ175	HEA 1	HEA 2	HEA 3	HEA 4	HEA 5
MTOW	-1.67%	0% (84050 lb)	-1.01%	-2.01%	-2.98%	5.65%	12.17%
OEW	-1.61%	0% (48161 lb)	-1.67%	-3.32%	-4.92%	4.95%	10.67%
Fuel Burn	0.22%	0% (18036 lb)	-1.07%	-2.13%	-3.15%	4.78%	10.30%

Table 23 Model comparisons between the representative ERJ175, the sized ERJ175, and its configurations for 0.5 kWh/kg specific energy, 1000 nmi range.

	ERJ175	Sized ERJ175	HEA 1	HEA 2	HEA 3	HEA 4	HEA 5
MTOW	18.51%	0% (67370 lb)	-0.82%	-1.62%	-2.43%	4.63%	9.48%
OEW	18.56%	0% (38603 lb)	-1.48%	-2.94%	-4.38%	3.93%	8.02%
Fuel Burn	39.62%	0% (10913 lb)	-0.91%	-1.80%	-2.69%	3.44%	6.97%

References

[1] International Energy Agency, "World air passenger traffic evolution, 1980-2020," *IEA, Paris*, 2022. URL `https://www.iea.org/data-and-statistics/charts/world-air-passenger-traffic-evolution-1980-2020`.

[2] International Civil Aviation Organization, "Report on the Feasibility of a Long-Term Aspirational Goal (LTAG) for International Civil Aviation CO2 Emission Reductions," Report, International Civil Aviation Organization, 2022.

[3] International Energy Agency, "The Future of Hydrogen," Report, International Energy Agency, 2019. URL `https://www.iea.org/reports/the-future-of-hydrogen`.

[4] Rendón, M. A., Sánchez R., C. D., Gallo M., J., and Anzai, A. H., "Aircraft Hybrid-Electric Propulsion: Development Trends, Challenges and Opportunities," *Journal of Control, Automation and Electrical Systems*, Vol. 32, No. 5, 2021, pp. 1244–1268. https://doi.org/10.1007/s40313-021-00740-x.

[5] Hepperle, M., "Electric Flight – Potential and Limitations," Tech. rep., NATO Science and Technology Organization, 2012.

[6] Geiß, I., "Sizing of the energy storage system of hybrid-electric aircraft in general aviation," *CEAS Aeronautical Journal*, Vol. 8, No. 1, 2017, pp. 53–65. https://doi.org/10.1007/s13272-016-0220-5.

[7] Pastra, C. L., Dull, C., Berumen, R., Yumuk, C., Cinar, G., and Mavris, D. N., "Viability Study of an Electrified Regional Turboprop," *2022 IEEE Transportation Electrification Conference & Expo (ITEC)*, 2022, pp. 231–236. https://doi.org/10.1109/ITEC53557.2022.9813756.

[8] Friedrich, C., and Robertson, P. A., "Hybrid-electric propulsion for aircraft," *Journal of Aircraft*, Vol. 52, No. 1, 2015, pp. 176–189.

[9] Finger, D. F., de Vries, R., Vos, R., Braun, C., and Bil, C., "Cross-Validation of Hybrid-Electric Aircraft Sizing Methods," *Journal of Aircraft*, 2022, pp. 1–19.

[10] Hoogreef, M., Vos, R., de Vries, R., and Veldhuis, L., "Conceptual Assessment of Hybrid Electric Aircraft with Distributed Propulsion and Boosted Turbofans," 2019. https://doi.org/10.2514/6.2019-1807.

[11] Cinar, G., Cai, Y., Chakraborty, I., and Mavris, D. N., "Sizing and optimization of novel general aviation vehicles and propulsion system architectures," *2018 Aviation Technology, Integration, and Operations Conference*, 2018, p. 3974.

[12] Finger, D., Braun, C., and Bil, C., "A Review of Configuration Design for Distributed Propulsion Transitioning VTOL Aircraft," 2017.

[13] Finger, D., Braun, C., and Bil, C., "An Initial Sizing Methodology for Hybrid-Electric Light Aircraft," 2018. https://doi.org/10.2514/6.2018-4229.

[14] Cinar, G., "A Methodology for Dynamic Sizing of Electric Power Generation and Distribution Architectures," Ph.D. thesis, Georgia Institute of Technology, 2018.

[15] Wroblewski, G. E., and Ansell, P. J., "Mission Analysis and Emissions for Conventional and Hybrid-Electric Commercial Transport Aircraft," 2019.

[16] Geiss, I., Notter, S., Strohmayer, A., and Fichter, W., "Optimized operation strategies for serial hybrid-electric aircraft," *2018 Aviation Technology, Integration, and Operations Conference*, 2018, p. 4230.

[17] Cinar, G., Cai, Y., Bendarkar, M. V., Burrell, A. I., Denney, R. K., and Mavris, D. N., "System analysis and design space exploration of regional aircraft with electrified powertrains," *Journal of Aircraft*, Vol. 60, No. 2, 2023, pp. 382–409.

[18] Cinar, G., Cai, Y., Denney, R. K., and Mavris, D. N., "Modeling and Simulation of a Parallel Hybrid Electric Regional Aircraft for the Electrified Powertrain Flight Demonstration (EPFD) Program," *2022 IEEE Transportation Electrification Conference & Expo (ITEC)*, IEEE, 2022, pp. 670–675.

[19] Hoelzen, J., Liu, Y., Bensmann, B., Winnefeld, C., Elham, A., Friedrichs, J., and Hanke-Rauschenbach, R., "Conceptual design of operation strategies for hybrid electric aircraft," *Energies*, Vol. 11, No. 1, 2018, p. 217.

[20] Shi, M., Cinar, G., and Mavris, D. N., "Fleet Analysis of a Hybrid Turboelectric Commercial Regional Jet under NASA ULI Program," *2021 AIAA/IEEE Electric Aircraft Technologies Symposium (EATS)*, 2021, pp. 1–22. https://doi.org/10.23919/EATS52162.2021.9704830.

[21] Jain, S., and Crossley, W. A., "Predicting Fleet-level Carbon Emission Reductions from Future Single-Aisle Hybrid Electric Aircraft," *2020 AIAA/IEEE Electric Aircraft Technologies Symposium (EATS)*, IEEE, 2020, pp. 1–15.

[22] Scholz, A. E., Michelmann, J., and Hornung, M., "Design, Operational and Environmental Assessment of a Hybrid-Electric Aircraft," *AIAA Scitech 2021 Forum*, 2021, p. 0259.

[23] Graver, B., Zhang, K., and Rutherford, D., "CO2 emissions from commercial aviation, 2018," *International Council on Clean Transportation*, Vol. 2019, 2019.

[24] Bureau of Transportation Statistics, "Air Carriers : T-100 Domestic Segment (U.S. Carriers)," , 2019. URL https://transtats.bts.gov/DL_SelectFields.aspx?gnoyr_VQ=FIM&QO_fu146_anzr=Nv4%20Pn44vr45.

[25] Cook, G. N., and Goodwin, J., "Airline networks: A comparison of hub-and-spoke and point-to-point systems," *Journal of Aviation/Aerospace Education & Research*, Vol. 17, No. 2, 2008, p. 1.

[26] Thomas, I., "United Airlines is aiming to have electric planes flying by 2030," , Oct 2022. URL https://www.cnbc.com/2022/10/06/united-airlines-is-aiming-to-have-electric-planes-flying-by-2030.html.

[27] Air Canada, "Air Canada to acquire 30 ES-30 electric regional aircraft from Heart Aerospace," , Sep 2022. URL https://www.newswire.ca/news-releases/air-canada-to-acquire-30-es-30-electric-regional-aircraft-from-heart-aerospace-873505575.html.

[28] Bureau of Transportation Statistics, "On-Time : Reporting Carrier On-Time Performance (1987-present)," , 2019. URL https://www.transtats.bts.gov/DL_SelectFields.aspx?gnoyr_VQ=FGJ&QO_fu146_anzr=b0-gvzr.

[29] Bris, G. L., Nguyen, L. G., Tagoe, B., Jonat, P., Justin, C., Reindel, E., Preston, K., and Ansell, P., "Preparing Your Airport for Electric Aircraft and Hydrogen Technologies," Report, Airport Cooperative Research Program, 2022.

[30] Anderson, J. D., *Aircraft Performance and Design*, McGraw-Hill, 1999.

[31] "Embraer 175: Airport Planning Manual," , 09 2015. URL https://www.embraercommercialaviation.com/wp-content/uploads/2017/02/APM_E175.pdf.

[32] Spierling, T., and Lents, C., "Parallel hybrid propulsion system for a regional turboprop: conceptual design and benefits analysis," *2019 AIAA/IEEE Electric Aircraft Technologies Symposium (EATS)*, IEEE, 2019, pp. 1–7. https://doi.org/10.2514/6.2019-4466.

[33] Eskenazi, A. G., Joshi, A. P., Butler, L. G., and Ryerson, M. S., "Equitable optimization of US airline route networks," *Computers, Environment and Urban Systems*, Vol. 102, 2023, p. 101973.